

A PRACTICAL GUIDE TO STOCHASTIC SIMULATIONS OF REACTION-DIFFUSION PROCESSES

RADEK ERBAN*, S. JONATHAN CHAPMAN*, AND PHILIP K. MAINI*

Abstract. A practical introduction to stochastic modelling of reaction-diffusion processes is presented. No prior knowledge of stochastic simulations is assumed. The methods are explained using illustrative examples. The article starts with the classical Gillespie algorithm for the stochastic modelling of chemical reactions. Then stochastic algorithms for modelling molecular diffusion are given. Finally, basic stochastic reaction-diffusion methods are presented. The connections between stochastic simulations and deterministic models are explained and basic mathematical tools (e.g. chemical master equation) are presented. The article concludes with an overview of more advanced methods and problems.

Key words. stochastic simulations, reaction-diffusion processes

AMS subject classifications. 60G05, 92C40, 60J60, 92C15

1. Introduction. There are two fundamental approaches to the mathematical modelling of chemical reactions and diffusion: *deterministic* models which are based on differential equations; and *stochastic* simulations. Stochastic models provide a more detailed understanding of the reaction-diffusion processes. Such a description is often necessary for the modelling of biological systems where small molecular abundances of some chemical species make deterministic models inaccurate or even inapplicable. Stochastic models are also necessary when biologically observed phenomena depend on stochastic fluctuations (e.g. switching between two favourable states of the system).

In this paper, we provide an accessible introduction for students to the stochastic modelling of the reaction-diffusion processes. We assume that students have a basic understanding of differential equations but we do not assume any prior knowledge of advanced probability theory or stochastic analysis. We explain stochastic simulation methods using illustrative examples. We also present basic theoretical tools which are used for analysis of stochastic methods. We start with a stochastic model of a single chemical reaction (degradation) in Section 2.1, introducing a basic stochastic simulation algorithm (SSA) and a mathematical equation suitable for its analysis (the so-called chemical master equation). Then we study systems of chemical reactions in the rest of Section 2, presenting the Gillespie SSA and some additional theoretical concepts. We introduce new theory whenever it provides more insights into the particular example. We believe that such an example-based approach is more accessible for students than introducing the whole theory first. In Section 3, we study SSAs for modelling diffusion of molecules. We focus on models of diffusion which are later used for the stochastic modelling of reaction-diffusion processes. Such methods are presented in Section 4. We also introduce further theoretical concepts, including the reaction-diffusion master equation, the Smoluchowski equation and the Fokker-Planck equation. We conclude with Sections 5 and 6 where more advanced problems, methods and theory are discussed, giving references suitable for further reading.

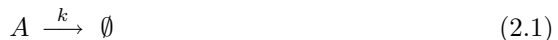
The stochastic methods and the corresponding theory are explained using several illustrative examples. We do not assume a prior knowledge of a particular computer language in this paper. A student might use any computer language to implement the examples from this paper. However, we believe that some students might benefit from

*University of Oxford, Mathematical Institute, 24-29 St. Giles', Oxford, OX1 3LB, United Kingdom; e-mails: erban@maths.ox.ac.uk, chapman@maths.ox.ac.uk, maini@maths.ox.ac.uk.

our computer codes which were used to compute the illustrative results in this paper. The computer codes (in Matlab or Fortran) can be downloaded from the website <http://www.maths.ox.ac.uk/cmb/Education/> which is hosted by the Centre for Mathematical Biology in the Mathematical Institute, University of Oxford.

2. Stochastic simulation of chemical reactions. The goal of this section is to introduce stochastic methods for the modelling of (spatially homogeneous) systems of chemical reactions. We present the Gillespie SSA, the chemical master equation and its consequences [18, 19]. We start with the simplest case possible, that of modelling a single chemical reaction, in Section 2.1. We then study two simple systems of chemical reactions in Sections 2.2 and 2.3.

2.1. Stochastic simulation of degradation. Let us consider the single chemical reaction



where A is the chemical species of interest and k is the rate constant of the reaction. The symbol \emptyset denotes chemical species which are of no further interest in what follows. The rate constant k in (2.1) is defined so that $k dt$ gives the probability that a randomly chosen molecule of chemical species A reacts (is degraded) during the time interval $[t, t + dt]$ where t is time and dt an (infinitesimally) small time step. In particular, the probability that exactly one reaction (2.1) occurs during the infinitesimal time interval $[t, t + dt]$ is equal to $A(t)k dt$ where we denote the number of molecules of chemical species A at time t simply as $A(t)$. This notational convention will be used throughout the paper.

Let us assume that we have n_0 molecules of A in the system at time $t = 0$, i.e. $A(0) = n_0$. Our first goal is to compute the number of molecules $A(t)$ for times $t > 0$. To do that, we need a computer routine generating random numbers uniformly distributed in the interval $(0, 1)$. Such a program is included in many modern programming languages (e.g. function `rand` in Matlab): It generates a number $r \in (0, 1)$, so that the probability that r is in a subinterval $(a, b) \subset (0, 1)$ is equal to $b - a$ for any $a, b \in (0, 1)$, $a < b$.

The mathematical definition of the chemical reaction (2.1) can be directly used to design a “naive” SSA for simulating it. We choose a small time step Δt . We compute the number of molecules $A(t)$ at times $t = i\Delta t$, $i = 1, 2, 3, \dots$, as follows. Starting with $t = 0$ and $A(0) = n_0$, we perform two steps at time t :

- (a1) Generate a random number r uniformly distributed in the interval $(0, 1)$.
- (b1) If $r < A(t)k \Delta t$, then put $A(t + \Delta t) = A(t) - 1$; otherwise, $A(t + \Delta t) = A(t)$. Then continue with step (a1) for time $t + \Delta t$.

Since r is a random number uniformly distributed in the interval $(0, 1)$, the probability that $r < A(t)k \Delta t$ is equal to $A(t)k \Delta t$. Consequently, step (b1) says that the probability that the chemical reaction (2.1) occurs in the time interval $[t, t + \Delta t]$ is equal to $A(t)k \Delta t$. Thus step (b1) correctly implements the definition of (2.1) provided that Δt is small. The time evolution of A obtained by the “naive” SSA (a1)–(b1) is given in Figure 2.1(a) for $k = 0.1 \text{ sec}^{-1}$, $A(0) = 20$ and $\Delta t = 0.005 \text{ sec}$. We repeated the stochastic simulation twice and we plotted two realizations of SSA (a1)–(b1). We see in Figure 2.1(a) that two realizations of SSA (a1)–(b1) give two different results. Each time we run the algorithm, we obtain different results. This is generally true for any SSA. Therefore, one might ask what useful and reproducible information can

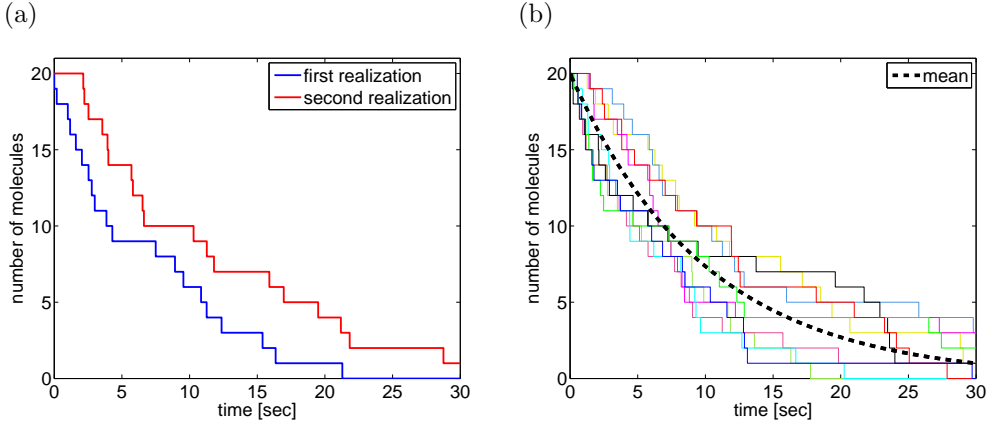


FIG. 2.1. Stochastic simulation of chemical reaction (2.1) for $k = 0.1 \text{ sec}^{-1}$ and $A(0) = 20$. (a) Number of molecules of A as a function of time for two realizations of the “naive” SSA (a1)–(b1) for $\Delta t = 0.005 \text{ sec}$; (b) results of ten realizations of SSA (a2)–(c2) (solid lines; different colours show different realizations) and stochastic mean (2.8) plotted by the dashed line.

be obtained from stochastic simulations? This question will be addressed later in this section.

The probability that exactly one reaction (2.1) occurs during the infinitesimal time interval $[t, t + dt]$ is equal to $A(t)k dt$. To design the SSA (a1)–(b1), we replaced dt by the finite time step Δt . In order to get reasonably accurate results, we must ensure that $A(t)k \Delta t \ll 1$ during the simulation. We used $k = 0.1 \text{ sec}^{-1}$ and $\Delta t = 0.005 \text{ sec}$. Since $A(t) \leq A(0) = 20$ for any $t \geq 0$, we have that $A(t)k \Delta t \in [0, 0.01]$ for any $t \geq 0$. Consequently, the condition $A(t)k \Delta t \ll 1$ is reasonably satisfied during the simulation. We might further increase the accuracy of the SSA (a1)–(b1) by decreasing Δt . However, decreasing Δt increases the computational intensity of the algorithm. The probability that the reaction (2.1) occurs during the time interval $[t, t + \Delta t]$ is less or equal to 1% for our parameter values. During most of the time steps, we generate a random number r in step (a1) to find out that no reaction occurs in step (b1). Hence, we need to generate a lot of random numbers before the reaction takes place. Our next task will be to design a more efficient method for the simulation of the chemical reaction (2.1). We will need only one random number to decide when the next reaction occurs. Moreover, the method will be exact. There will be no approximation in the derivation of the following SSA (a2)–(c2).

Suppose that there are $A(t)$ molecules at time t in the system. Our goal is to compute time $t + \tau$ when the next reaction (2.1) takes place. Let us denote by $f(A(t), s) ds$ the probability that, given $A(t)$ molecules at time t in the system, the next reaction occurs during the time interval $[t + s, t + s + ds]$ where ds is an (infinitesimally) small time step. Let $g(A(t), s)$ be the probability that no reaction occurs in interval $[t, t + s]$. Then the probability $f(A(t), s) ds$ can be computed as a product of $g(A(t), s)$ and the probability that a reaction occurs in the time interval $[t + s, t + s + ds]$ which is given according to the definition of (2.1) by $A(t + s)k ds$. Thus we have

$$f(A(t), s) ds = g(A(t), s) A(t + s) k ds.$$

Since no reaction occurs in $[t, t + s]$, we have $A(t + s) = A(t)$. This implies

$$f(A(t), s) ds = g(A(t), s) A(t) k ds. \quad (2.2)$$

To compute the probability $g(A(t), s)$, let us consider $\sigma > 0$. The probability that no reaction occurs in the interval $[t, t + \sigma + d\sigma)$ can be computed as the product of the probability that no reaction occurs in the interval $[t, t + \sigma)$ and the probability that no reaction occurs in the interval $[t + \sigma, t + \sigma + d\sigma)$. Hence

$$g(A(t), \sigma + d\sigma) = g(A(t), \sigma)[1 - A(t + \sigma)k d\sigma].$$

Since no reaction occurs in the interval $[t, t + \sigma)$, we have $A(t + \sigma) = A(t)$. Consequently,

$$\frac{g(A(t), \sigma + d\sigma) - g(A(t), \sigma)}{d\sigma} = -A(t)k g(A(t), \sigma).$$

Passing to the limit $d\sigma \rightarrow 0$, we obtain the ordinary differential equation (in the σ variable)

$$\frac{dg(A(t), \sigma)}{d\sigma} = -A(t)k g(A(t), \sigma).$$

Solving this equation with initial condition $g(A(t), 0) = 1$, we obtain

$$g(A(t), \sigma) = \exp[-A(t)k\sigma].$$

Consequently, (2.2) can be written as

$$f(A(t), s) ds = A(t)k \exp[-A(t)ks] ds. \quad (2.3)$$

Our goal is to find τ such that $t + \tau$ is the time when the next reaction occurs, provided that there are $A(t)$ molecules of A in the system at time t . Such $\tau \in (0, \infty)$ is a random number which has to be generated consistently with the definition of the chemical reaction (2.1). To do that, we consider the function $F(\cdot)$ defined by

$$F(\tau) = \exp[-A(t)k\tau]. \quad (2.4)$$

The function $F(\cdot)$ is monotone decreasing for $A(t) > 0$. If τ is a random number from the interval $(0, \infty)$, then $F(\tau)$ is a random number from the interval $(0, 1)$. If τ is a random number chosen consistently with the reaction (2.1), then $F(\tau)$ is a random number uniformly distributed in the interval $(0, 1)$ which can be shown as follows. Let $a, b, a < b$, be chosen arbitrarily in the interval $(0, 1)$. The probability that $F(\tau) \in (a, b)$ is equal to the probability that $\tau \in (F^{-1}(b), F^{-1}(a))$ which is given by the integral of $f(A(t), s)$ over s in the interval $(F^{-1}(b), F^{-1}(a))$. Using (2.3) and (2.4), we obtain

$$\begin{aligned} \int_{F^{-1}(b)}^{F^{-1}(a)} f(A(t), s) ds &= \int_{F^{-1}(b)}^{F^{-1}(a)} A(t)k \exp[-A(t)ks] ds \\ &= - \int_{F^{-1}(b)}^{F^{-1}(a)} \frac{dF}{ds} ds = -F[F^{-1}(a)] + F[F^{-1}(b)] = b - a. \end{aligned}$$

Hence we have verified that $F(\tau)$ is a random number uniformly distributed in $(0, 1)$. Such a number can be obtained using the random number generator (e.g. function

`rand` in Matlab). Let us denote it by r . The previous observation implies that we can generate the time step τ by putting $r = F(\tau)$. Using (2.4), we obtain

$$r = \exp[-A(t)k\tau].$$

Solving for τ , we obtain the formula

$$\tau = \frac{1}{A(t)k} \ln \left[\frac{1}{r} \right]. \quad (2.5)$$

Consequently, the SSA for the chemical reaction (2.1) can be written as follows. Starting with $t = 0$ and $A(0) = n_0$, we perform three steps at time t :

- (a2) Generate a random number r uniformly distributed in the interval $(0, 1)$.
- (b2) Compute the time when the next reaction (2.1) occurs as $t + \tau$ where τ is given by (2.5).
- (c2) Compute the number of molecules at time $t + \tau$ by $A(t + \tau) = A(t) - 1$.
Then continue with step (a2) for time $t + \tau$.

Steps (a2)–(c2) are repeated until we reach the time when there is no molecule of A in the system, i.e. $A = 0$. SSA (a2)–(c2) computes the time of the next reaction $t + \tau$ using formula (2.5) in step (b2) with the help of one random number only. Then the reaction is performed in step (c2) by decreasing the number of molecules of chemical species A by 1. The time evolution of A obtained by SSA (a2)–(c2) is given in Figure 2.1(b). We plot ten realizations of SSA (a2)–(c2) for $k = 0.1 \text{ sec}^{-1}$ and $A(0) = 20$. Since the function $A(t)$ has only integer values $\{0, 1, 2, \dots, 20\}$, it is not surprising that some of the computed curves $A(t)$ partially overlap. On the other hand, all ten realizations yield different functions $A(t)$. Even if we made millions of stochastic realizations, it would be very unlikely (with probability zero) that there would be two realizations giving exactly the same results. Therefore, the details of one realization $A(t)$ are of no special interest (they depend on the sequence of random numbers obtained by the random number generator). However, averaging values of A at time t over many realizations (e.g. computing the stochastic mean of A), we obtain a reproducible characteristic of the system – see the dashed line in Figure 2.1(b). The stochastic mean of $A(t)$ over (infinitely) many realizations can be also computed theoretically as follows.

Let us denote by $p_n(t)$ the probability that there are n molecules of A at time t in the system, i.e. $A(t) = n$. Let us consider an (infinitesimally) small time step dt chosen such that the probability that two molecules are degraded during $[t, t + dt)$ is negligible compared to the probability that only one molecule is degraded during $[t, t + dt)$. Then there are two possible ways for $A(t + dt)$ to take the value n : either $A(t) = n$ and no reaction occurred in $[t, t + dt)$, or $A(t) = n + 1$ and one molecule was degraded in $[t, t + dt)$. Hence

$$p_n(t + dt) = p_n(t) \times (1 - kn \, dt) + p_{n+1}(t) \times k(n + 1) \, dt.$$

A simple algebraic manipulation yields

$$\frac{p_n(t + dt) - p_n(t)}{dt} = k(n + 1) p_{n+1}(t) - kn p_n(t).$$

Passing to the limit $dt \rightarrow 0$, we obtain the so-called *chemical master equation* in the form

$$\frac{dp_n}{dt} = k(n + 1) p_{n+1} - kn p_n. \quad (2.6)$$

Equation (2.6) looks like an infinite system of ordinary differential equations (ODEs) for p_n , $n = 0, 1, 2, 3, \dots$. Our initial condition $A(0) = n_0$ implies that there are never more than n_0 molecules in the system. Consequently, $p_n \equiv 0$ for $n > n_0$ and the system (2.6) reduces to a system of $(n_0 + 1)$ ODEs for p_n , $n \leq n_0$. The equation for $n = n_0$ reads as follows

$$\frac{dp_{n_0}}{dt} = -kn_0 p_{n_0}.$$

Solving this equation with initial condition $p_{n_0}(0) = 1$, we get $p_{n_0}(t) = \exp[-kn_0 t]$. Using this formula in the chemical master equation (2.6) for $p_{n_0-1}(t)$, we obtain

$$\frac{d}{dt} p_{n_0-1}(t) = kn_0 \exp[-kn_0 t] - k(n_0 - 1) p_{n_0-1}(t).$$

Solving this equation with initial condition $p_{n_0-1}(0) = 0$, we obtain $p_{n_0-1}(t) = \exp[-k(n_0 - 1)t] n_0(1 - \exp[-kt])$. Using mathematical induction, it is possible to show

$$p_n(t) = \exp[-knt] \binom{n_0}{n} \{1 - \exp[-kt]\}^{n_0-n}. \quad (2.7)$$

The formula (2.7) provides all the information about the stochastic process which is defined by (2.1) and initial condition $A(0) = n_0$. We can never say for sure that $A(t) = n$; we can only say that $A(t) = n$ with probability $p_n(t)$. In particular, formula (2.7) can be used to derive a formula for the mean value of $A(t)$ over (infinitely) many realizations, which is defined by

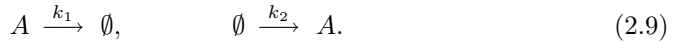
$$M(t) = \sum_{n=0}^{n_0} n p_n(t).$$

Using (2.7), we deduce

$$\begin{aligned} M(t) &= \sum_{n=0}^{n_0} n p_n(t) = \sum_{n=0}^{n_0} n \exp[-knt] \binom{n_0}{n} \{1 - \exp[-kt]\}^{n_0-n} \\ &= n_0 \exp[-kt] \sum_{n=1}^{n_0} \binom{n_0-1}{n-1} \{1 - \exp[-kt]\}^{(n_0-1)-(n-1)} \{\exp[-kt]\}^{n-1} \\ &= n_0 \exp[-kt]. \end{aligned} \quad (2.8)$$

The chemical master equation (2.6) and its solution (2.7) can be also used to quantify the stochastic fluctuations around the mean value (2.8), i.e. how much can an individual realization of SSA (a2)–(c2) differ from the mean value given by (2.8). We will present the corresponding theory and results on a more complicated illustrative example in Section 2.2. Finally, let us note that a classical deterministic description of the chemical reaction (2.1) is given by the ODE $da/dt = -ka$. Solving this equation with initial condition $a(0) = n_0$, we obtain the function (2.8), i.e. the stochastic mean is equal to the solution of the corresponding deterministic ODE. However, we should emphasize that this is not true for general systems of chemical reactions, as we will see in Section 2.3 and Section 5.1.

2.2. Stochastic simulation of production and degradation. We consider a system of two chemical reactions



The first reaction describes the degradation of chemical A with the rate constant k_1 . It was already studied previously as reaction (2.1). We couple it with the second reaction which represents the production of chemical A with the rate constant k_2 . The exact meaning of the second chemical reaction in (2.9) is that one molecule of A is created during the time interval $[t, t + dt)$ with probability $k_2 dt$. As before, the symbol \emptyset denotes chemical species which are of no special interest to the modeller. The impact of other chemical species on the rate of production of A is assumed to be time independent and is already incorporated in the rate constant k_2 . To simulate the system of chemical reactions (2.9), we perform the following four steps at time t (starting with $A(0) = n_0$ at time $t = 0$):

- (a3) Generate two random numbers r_1, r_2 uniformly distributed in $(0, 1)$.
- (b3) Compute $\alpha_0 = A(t)k_1 + k_2$.
- (c3) Compute the time when the next chemical reaction takes place as $t + \tau$ where

$$\tau = \frac{1}{\alpha_0} \ln \left[\frac{1}{r_1} \right]. \quad (2.10)$$

- (d3) Compute the number of molecules at time $t + \tau$ by

$$A(t + \tau) = \begin{cases} A(t) + 1 & \text{if } r_2 < k_2/\alpha_0; \\ A(t) - 1 & \text{if } r_2 \geq k_2/\alpha_0. \end{cases} \quad (2.11)$$

Then continue with step (a3) for time $t + \tau$.

To justify that SSA (a3)–(d3) correctly simulates (2.9), let us note that the probability that any of the reactions in (2.9) takes place in the time interval $[t, t + dt)$ is equal to $\alpha_0 dt$. It is given as a sum of the probability that the first reaction occurs ($A(t)k_1 dt$) and the probability that the second reaction occurs ($k_2 dt$). Formula (2.10) gives the time $t + \tau$ when the next reaction takes place. It can be justified using the same arguments as for formula (2.5). Once we know the time $t + \tau$, a molecule is produced with probability k_2/α_0 , i.e. the second reaction in (2.9) takes place with probability k_2/α_0 . Otherwise, a molecule is degraded, i.e. the first reaction in (2.9) occurs. The decision as to which reaction takes place is given in step (d3) with the help of the second uniformly distributed random number r_2 .

Five realizations of SSA (a3)–(d3) are presented in Figure 2.2(a) as solid lines. We plot the number of molecules of A as a function of time for $A(0) = 0$, $k_1 = 0.1 \text{ sec}^{-1}$ and $k_2 = 1 \text{ sec}^{-1}$. We see that, after an initial transient, the number of molecules $A(t)$ fluctuates around its mean value. To compute the stochastic mean and quantify the stochastic fluctuations, we use the chemical master equation which can be written for the chemical system (2.9) in the following form

$$\frac{dp_n}{dt} = k_1(n+1)p_{n+1} - k_1 n p_n + k_2 p_{n-1} - k_2 p_n \quad (2.12)$$

where $p_n(t)$ denotes the probability that $A(t) = n$ for $n = 0, 1, 2, 3, \dots$. Let us note that the third term on the right hand side is missing in (2.12) for $n = 0$; i.e. we use

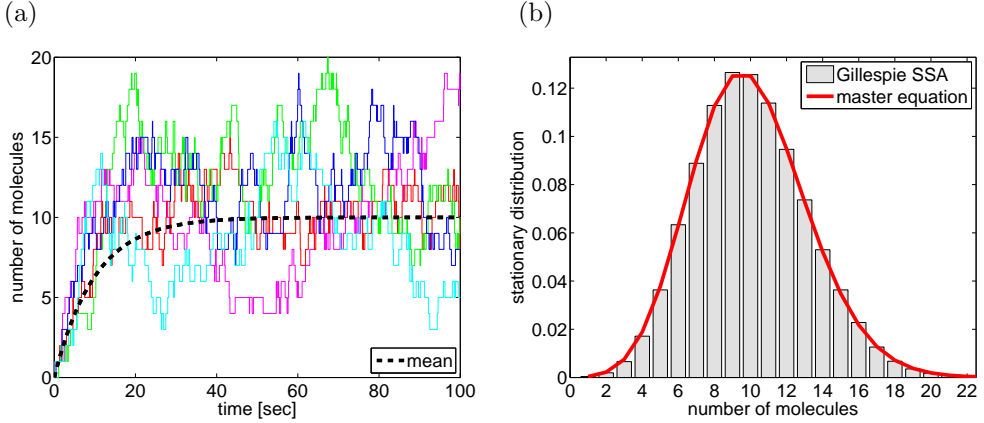


FIG. 2.2. *Stochastic simulation of the system of chemical reactions (2.9) for $A(0) = 0$, $k_1 = 0.1 \text{ sec}^{-1}$ and $k_2 = 1 \text{ sec}^{-1}$. (a) $A(t)$ given by five realizations of SSA (a3)–(d3) (solid lines) and stochastic mean (dashed line). (b) Stationary distribution $\phi(n)$ obtained by long time simulation of SSA (a3)–(d3) (gray histogram) and by formulae (2.21)–(2.22) (red solid line).*

the convention that $p_{-1} \equiv 0$. The first two terms on the right hand side correspond to the first reaction in (2.9). They already appeared in equation (2.6). Production of A is described by the third and fourth term on the right hand side of (2.9). To derive the chemical master equation (2.12), we can use similar arguments as in the derivation of (2.6). The stochastic mean $M(t)$ and variance $V(t)$ are defined by

$$M(t) = \sum_{n=0}^{\infty} n p_n(t), \quad V(t) = \sum_{n=0}^{\infty} (n - M(t))^2 p_n(t). \quad (2.13)$$

The stochastic mean $M(t)$ gives the average number of molecules of A at time t , while the variance $V(t)$ describes the fluctuations. In Section 2.1, we first solved the chemical master equation (2.6) and then we used its solution (2.7) to compute $M(t)$. Alternatively, we could use the chemical master equation to derive an evolution equation for $M(t)$, i.e. we could find $M(t)$ without solving the chemical master equation. Such an approach will be presented in this section. Multiplying (2.12) by n and summing over n , we obtain

$$\frac{d}{dt} \sum_{n=0}^{\infty} n p_n = k_1 \sum_{n=0}^{\infty} n(n+1) p_{n+1} - k_1 \sum_{n=0}^{\infty} n^2 p_n + k_2 \sum_{n=1}^{\infty} n p_{n-1} - k_2 \sum_{n=0}^{\infty} n p_n.$$

Using definition (2.13) on the left hand side and changing indices $n+1 \rightarrow n$ (resp. $n-1 \rightarrow n$) in the first (resp. third) sum on the right hand side, we obtain

$$\frac{dM}{dt} = k_1 \sum_{n=0}^{\infty} (n-1)n p_n - k_1 \sum_{n=0}^{\infty} n^2 p_n + k_2 \sum_{n=0}^{\infty} (n+1) p_n - k_2 \sum_{n=0}^{\infty} n p_n.$$

Adding the first and the second sum (resp. the third and the fourth sum) on the right hand side, we get

$$\frac{dM}{dt} = -k_1 \sum_{n=0}^{\infty} n p_n + k_2 \sum_{n=0}^{\infty} p_n. \quad (2.14)$$

Since $p_n(t)$ is the probability that $A(t) = n$ and $A(t)$ is equal to a nonnegative integer with probability 1, we have

$$\sum_{n=0}^{\infty} p_n(t) = 1. \quad (2.15)$$

Using this fact together with the definition of $M(t)$, equation (2.14) implies the evolution equation for $M(t)$ in the form

$$\frac{dM}{dt} = -k_1 M + k_2. \quad (2.16)$$

The solution of (2.16) with initial condition $M(0) = 0$ is plotted as a dashed line in Figure 2.2(a). To derive the evolution equation for the variance $V(t)$, let us first observe that definition (2.13) implies

$$\sum_{n=0}^{\infty} n^2 p_n(t) = V(t) + M(t)^2. \quad (2.17)$$

Multiplying (2.12) by n^2 and summing over n , we obtain

$$\frac{d}{dt} \sum_{n=0}^{\infty} n^2 p_n = k_1 \sum_{n=0}^{\infty} n^2 (n+1) p_{n+1} - k_1 \sum_{n=0}^{\infty} n^3 p_n + k_2 \sum_{n=1}^{\infty} n^2 p_{n-1} - k_2 \sum_{n=0}^{\infty} n^2 p_n.$$

Changing indices $n+1 \rightarrow n$ (resp. $n-1 \rightarrow n$) in the first (resp. third) sum on the right hand side and adding the first and the second sum (resp. the third and the fourth sum) on the right hand side, we get

$$\frac{d}{dt} \sum_{n=0}^{\infty} n^2 p_n = k_1 \sum_{n=0}^{\infty} (-2n^2 + n) p_n + k_2 \sum_{n=0}^{\infty} (2n+1) p_n.$$

Using (2.17), (2.15) and (2.13), we obtain

$$\frac{dV}{dt} + 2M \frac{dM}{dt} = -2k_1 [V + M^2] + k_1 M + 2k_2 M + k_2.$$

Substituting (2.16) for dM/dt , we derive the evolution equation for the variance $V(t)$ in the following form

$$\frac{dV}{dt} = -2k_1 V + k_1 M + k_2. \quad (2.18)$$

The time evolution of $M(t)$ and $V(t)$ is described by (2.16) and (2.18). Let us define the stationary values of $M(t)$ and $V(t)$ by

$$M_s = \lim_{t \rightarrow \infty} M(t), \quad V_s = \lim_{t \rightarrow \infty} V(t). \quad (2.19)$$

The values of M_s and V_s can be computed using the steady state equations corresponding to (2.16) and (2.18), namely by solving

$$0 = -k_1 M_s + k_2, \quad \text{and} \quad 0 = -2k_1 V_s + k_1 M_s + k_2.$$

Consequently,

$$M_s = V_s = \frac{k_2}{k_1}.$$

For our parameter values $k_1 = 0.1 \text{ sec}^{-1}$ and $k_2 = 1 \text{ sec}^{-1}$, we obtain $M_s = V_s = 10$. We see in Figure 2.2(a) that $A(t)$ fluctuates after a sufficiently long time around the mean value $M_s = 10$. To quantify the fluctuations, one often uses the square root of V_s , the so-called mean standard deviation which is equal to $\sqrt{10}$.

More detailed information about the fluctuations is given by the so-called *stationary distribution* $\phi(n)$, $n = 0, 1, 2, 3, \dots$, which is defined as

$$\phi(n) = \lim_{t \rightarrow \infty} p_n(t). \quad (2.20)$$

This means that $\phi(n)$ is the probability that $A(t) = n$ after an (infinitely) long time. One way to compute $\phi(n)$ is to run SSA (a3)–(d3) for a long time and create a histogram of values of $A(t)$ at given time intervals. Using $k_1 = 0.1 \text{ sec}^{-1}$ and $k_2 = 1 \text{ sec}^{-1}$, the results of such a long time computation are presented in Figure 2.2(b) as a gray histogram. To compute it, we ran SSA (a3)–(d3) for 10^5 seconds, recording the value of $A(t)$ every second and then dividing the whole histogram by the number of recordings, i.e. by 10^5 . An alternative way to compute $\phi(n)$ is to use the steady state version of the chemical master equation (2.12), namely

$$\begin{aligned} 0 &= k_1 \phi(1) - k_2 \phi(0) \\ 0 &= k_1(n+1) \phi(n+1) - k_1 n \phi(n) + k_2 \phi(n-1) - k_2 \phi(n), \quad \text{for } n \geq 1, \end{aligned}$$

which implies

$$\phi(1) = \frac{k_2}{k_1} \phi(0), \quad (2.21)$$

$$\phi(n+1) = \frac{1}{k_1(n+1)} [k_1 n \phi(n) + k_2 \phi(n) - k_2 \phi(n-1)], \quad \text{for } n \geq 1. \quad (2.22)$$

Consequently, we can express $\phi(n)$ for any $n \geq 1$ in terms of $\phi(0)$. The formulae (2.21)–(2.22) yield an alternative way to compute $\phi(n)$. We put $\phi(0) = 1$ and we compute $\phi(n)$, for sufficiently many n , by (2.21)–(2.22). Then we divide $\phi(n)$, $n \geq 0$, by $\sum \phi(n)$. The results obtained by (2.21)–(2.22) are plotted in Figure 2.2(b) as a (red) solid line. As expected, the results compare well with the results obtained by the long time stochastic simulation.

We can also find the formula for $\phi(n)$ directly. We let a reader to verify that the solution of the recurrence formula (2.21)–(2.22) can be written as

$$\phi(n) = \frac{C}{n!} \left(\frac{k_2}{k_1} \right)^n \quad (2.23)$$

where C is a real constant. Using (2.15) and (2.20), we have

$$\sum_{n=0}^{\infty} \phi(n) = 1. \quad (2.24)$$

Substituting (2.23) into the normalization condition (2.24), we get

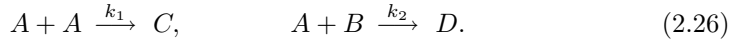
$$1 = \sum_{n=0}^{\infty} \frac{C}{n!} \left(\frac{k_2}{k_1} \right)^n = C \sum_{n=0}^{\infty} \frac{1}{n!} \left(\frac{k_2}{k_1} \right)^n = C \exp \left[\frac{k_2}{k_1} \right]$$

where we used the Taylor series for the exponential function to get the last equality. Consequently, $C = \exp[-k_2/k_1]$ which, together with (2.23), implies that the stationary distribution $\phi(n)$ is the Poisson distribution

$$\phi(n) = \frac{1}{n!} \left(\frac{k_2}{k_1} \right)^n \exp \left[-\frac{k_2}{k_1} \right]. \quad (2.25)$$

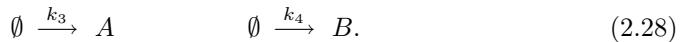
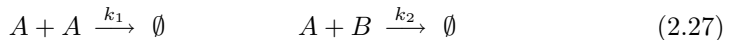
Thus the red solid line in Figure 2.2(b) which was obtained numerically by the recurrence formula (2.21)–(2.22) can be also viewed as the stationary distribution $\phi(n)$ given by the explicit exact formula (2.25).

2.3. Gillespie algorithm. SSAs (a2)–(c2) and (a3)–(d3) were special forms of the so-called Gillespie SSA. In this section, we present this algorithm for a more complicated illustrative example which will also involve second-order chemical reactions. Such chemical reactions are of the following form



In the first equation, two molecules of A react with rate constant k_1 to produce C . The probability that the reaction takes place in the time interval $[t, t + dt)$ is equal to $A(t)(A(t) - 1)k_1 dt$. We define the *propensity function* of the first reaction as $\alpha_1(t) = A(t)(A(t) - 1)k_1$. Then the probability that the first reaction occurs in the time interval $[t, t + dt)$ is equal to $\alpha_1(t) dt$. The propensity function which corresponds to the second equation in (2.26) is defined as $\alpha_2(t) = A(t)B(t)k_1$ and the probability that the second reaction occurs in the time interval $[t, t + dt)$ is equal to $\alpha_2(t) dt$. In such a case, one molecule of A and one molecule of B react to form a molecule of D . In general, the propensity function can be defined for any chemical reaction so that its product with dt gives the probability that the given reaction occurs in the infinitesimally small time interval $[t, t + dt)$.

We consider that A and B can react according to (2.26). Moreover, we assume that they are also produced with constant rates, that is, we consider a system of four chemical equations:



Let us note that we are not interested in chemical species C and D . Hence, we replaced them by \emptyset , consistent with our previous notation of unimportant chemical species. To simulate the system of chemical reactions (2.27)–(2.28), we perform the following four steps at time t (starting with $A(0) = n_0$, $B(0) = m_0$ at time $t = 0$):

- (a4) Generate two random numbers r_1, r_2 uniformly distributed in $(0, 1)$.
- (b4) Compute the propensity functions of each reaction by $\alpha_1 = A(t)(A(t) - 1)k_1$, $\alpha_2 = A(t)B(t)k_2$, $\alpha_3 = k_3$ and $\alpha_4 = k_4$. Compute $\alpha_0 = \alpha_1 + \alpha_2 + \alpha_3 + \alpha_4$.
- (c4) Compute the time when the next chemical reaction takes place as $t + \tau$ where

$$\tau = \frac{1}{\alpha_0} \ln \left[\frac{1}{r_1} \right]. \quad (2.29)$$

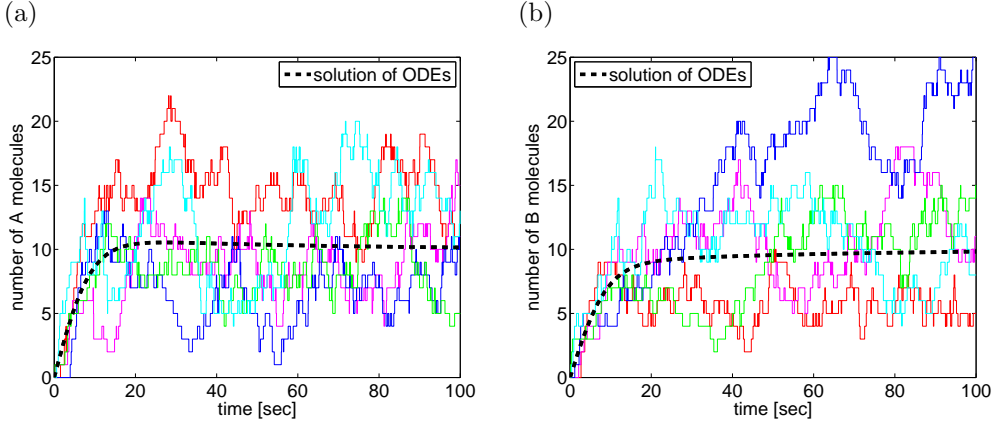


FIG. 2.3. Five realizations of SSA (a4)–(d4). Number of molecules of chemical species A (left panel) and B (right panel) are plotted as functions of time as solid lines. Different colours correspond to different realizations. The solution of (2.33)–(2.34) is given by the dashed line. We use $A(0) = 0$, $B(0) = 0$, $k_1 = 10^{-3} \text{ sec}^{-1}$, $k_2 = 10^{-2} \text{ sec}^{-1}$, $k_3 = 1.2 \text{ sec}^{-1}$ and $k_4 = 1 \text{ sec}^{-1}$.

(d4) Compute the number of molecules at time $t + \tau$ by

$$A(t + \tau) = \begin{cases} A(t) - 2 & \text{if } 0 \leq r_2 < \alpha_1/\alpha_0; \\ A(t) - 1 & \text{if } \alpha_1/\alpha_0 \leq r_2 < (\alpha_1 + \alpha_2)/\alpha_0; \\ A(t) + 1 & \text{if } (\alpha_1 + \alpha_2)/\alpha_0 \leq r_2 < (\alpha_1 + \alpha_2 + \alpha_3)/\alpha_0; \\ A(t) & \text{if } (\alpha_1 + \alpha_2 + \alpha_3)/\alpha_0 \leq r_2 < 1; \end{cases} \quad (2.30)$$

$$B(t + \tau) = \begin{cases} B(t) & \text{if } 0 \leq r_2 < \alpha_1/\alpha_0; \\ B(t) - 1 & \text{if } \alpha_1/\alpha_0 \leq r_2 < (\alpha_1 + \alpha_2)/\alpha_0; \\ B(t) & \text{if } (\alpha_1 + \alpha_2)/\alpha_0 \leq r_2 < (\alpha_1 + \alpha_2 + \alpha_3)/\alpha_0; \\ B(t) + 1 & \text{if } (\alpha_1 + \alpha_2 + \alpha_3)/\alpha_0 \leq r_2 < 1; \end{cases} \quad (2.31)$$

Then continue with step (a4) for time $t + \tau$.

SSA (a4)–(d4) is a direct generalisation of SSA (a3)–(d3). At each time step, we first ask the question when will the next reaction occur? The answer is given by formula (2.29) which can be justified using the same arguments as formulae (2.5) or (2.10). Then we ask the question which reaction takes place. The probability that the i -th chemical reaction occurs is given by α_i/α_0 . The decision which reaction takes place is given in step (d4) with the help of the second uniformly distributed random number r_2 . Knowing that the i -th reaction took place, we update the number of reactants and products accordingly. Results of five realizations of SSA (a4)–(d4) are plotted in Figure 2.3 as solid lines. We use $A(0) = 0$, $B(0) = 0$, $k_1 = 10^{-3} \text{ sec}^{-1}$, $k_2 = 10^{-2} \text{ sec}^{-1}$, $k_3 = 1.2 \text{ sec}^{-1}$ and $k_4 = 1 \text{ sec}^{-1}$. We plot the number of molecules of chemical species A and B as functions of time. We see that, after initial transients, $A(t)$ and $B(t)$ fluctuate around their average values. They can be estimated from long time stochastic simulations as 9.6 for A and 12.2 for B .

Let $p_{n,m}(t)$ be the probability that $A(t) = n$ and $B(t) = m$. The chemical master

equation can be written in the following form

$$\begin{aligned} \frac{dp_{n,m}}{dt} = & k_1(n+2)(n+1)p_{n+2,m} - k_1n(n-1)p_{n,m} \\ & + k_2(n+1)(m+1)p_{n+1,m+1} - k_2nm p_{n,m} \\ & + k_3p_{n-1,m} - k_3p_{n,m} + k_4p_{n,m-1} - k_4p_{n,m} \end{aligned} \quad (2.32)$$

for $n, m \geq 0$, with the convention that $p_{n,m} \equiv 0$ if $n < 0$ or $m < 0$. The first difference between (2.32) and the chemical master equations from the previous sections is that equation (2.32) is parametrised by two indices n and m . The second important difference is that (2.32) cannot be solved analytically as we did with (2.6). Moreover, it does not lead to closed evolution equations for stochastic means and variances; i.e. we cannot follow the same technique as in the case of equation (2.12). The approach from the previous section does not work. Let us note that the probability $p_{n,m}(t)$ is sometimes denoted by $p(n, m, t)$; such a notational convention is often used when we consider systems of many chemical species. We will use it in the following sections to avoid long subscripts.

The classical deterministic description of the chemical system (2.27)–(2.28) is given by the system of ODEs

$$\frac{da}{dt} = -2k_1a^2 - k_2ab + k_3, \quad (2.33)$$

$$\frac{db}{dt} = -k_2ab + k_4. \quad (2.34)$$

The solution of (2.33)–(2.34) with initial conditions $a(0) = 0$ and $b(0) = 0$ is plotted as a dashed line in Figure 2.3. Let us note that the equations (2.33)–(2.34) do not describe the stochastic means of $A(t)$ and $B(t)$. For example, the steady state values of (2.33)–(2.34) are (for the parameter values of Figure 2.3) equal to $a_s = b_s = 10$. On the other hand, the average values estimated from long time stochastic simulations are 9.6 for A and 12.2 for B . We will see later in Section 5.1 that the difference between the results of stochastic simulations and the corresponding ODEs can be even more significant.

The stationary distribution is defined by

$$\phi(n, m) = \lim_{t \rightarrow \infty} p_{n,m}(t).$$

This can be computed by long time simulations of SSA (a4)–(d4) and is plotted in Figure 2.4(a). We see that there is a correlation between the values of A and B . This can also be observed in Figure 2.3. Looking at the blue realizations, we see that the values of $A(t)$ are below the average and the values of $B(t)$ are above the average, similarly for other realizations. One can also define the stationary distribution of A only by

$$\phi(n) = \sum_{m=0}^{\infty} \phi(n, m). \quad (2.35)$$

Summing the results of Figure 2.4(a) over m , we obtain $\phi(n)$ which is plotted in Figure 2.4(b) as a gray histogram. The red bar highlights the steady state value $a_s = 10$ of system (2.33)–(2.34).

SSAs (a3)–(d3) and (a4)–(d4) were special forms of the so-called Gillespie SSA. To conclude this section, we formulate the Gillespie SSA in its full generality. Let us

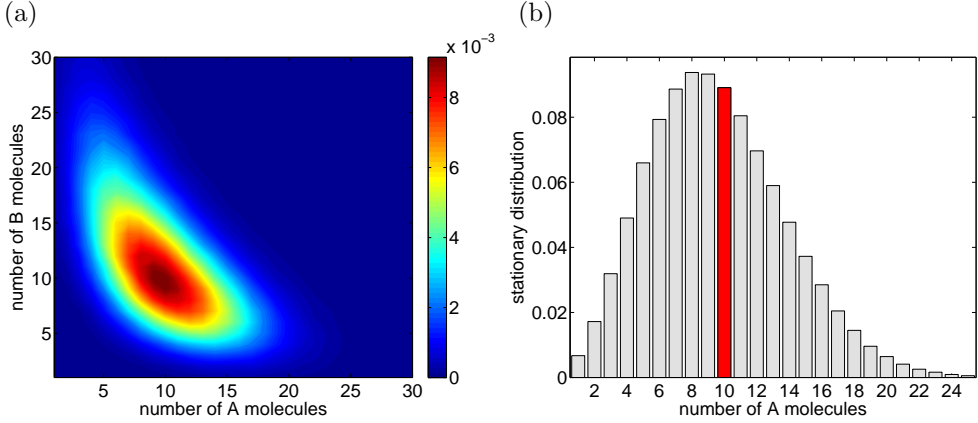


FIG. 2.4. (a) Stationary distribution $\phi(n, m)$ obtained by long time simulation of (a4)–(d4) for $k_1 = 10^{-3} \text{ sec}^{-1}$, $k_2 = 10^{-2} \text{ sec}^{-1}$, $k_3 = 1.2 \text{ sec}^{-1}$ and $k_4 = 1 \text{ sec}^{-1}$. (b) Stationary distribution of A obtained by (2.35).

consider that we have a system of q chemical reactions. Let $\alpha_i(t)$ be the propensity function of the i -th reaction, $i = 1, 2, \dots, q$, at time t , that is, $\alpha_i(t) dt$ is the probability that the i -th reaction occurs in the time interval $[t, t + dt)$. Then the Gillespie SSA consists of the following four steps at time t .

- (a5) Generate two random numbers r_1, r_2 uniformly distributed in $(0, 1)$.
- (b5) Compute the propensity function $\alpha_i(t)$ of each reaction. Compute

$$\alpha_0 = \sum_{i=1}^q \alpha_i(t). \quad (2.36)$$

- (c5) Compute the time when the next chemical reaction takes place as $t + \tau$ where τ is given by (2.29).
- (d5) Compute which reaction occurs at time $t + \tau$. Find j such that

$$r_2 \geq \frac{1}{\alpha_0} \sum_{i=1}^{j-1} \alpha_i \quad \text{and} \quad r_2 < \frac{1}{\alpha_0} \sum_{i=1}^j \alpha_i.$$

Then the j -th reaction takes place, i.e. update numbers of reactants and products of the j -th reaction.

Continue with step (a5) for time $t + \tau$.

The Gillespie SSA (a5)–(d5) provides an exact method for the stochastic simulation of systems of chemical reactions. It was applied previously as SSA (a2)–(c2) for the chemical reaction (2.1), as SSA (a3)–(d3) for the chemical system (2.9) and as SSA (a4)–(d4) for the chemical system (2.27)–(2.28). Our simple examples can be simulated quickly in Matlab (in less than a second on present-day computers). If one considers systems of many chemical reactions and many chemical species, then SSA (a5)–(d5) might be computationally intensive. In such a case, there are ways to make the Gillespie SSA more efficient. For example, it would be a waste of time to recompute all the propensity functions at each time step (step (b5)). We simulate one reaction per one time step. Therefore, it makes sense to update only those

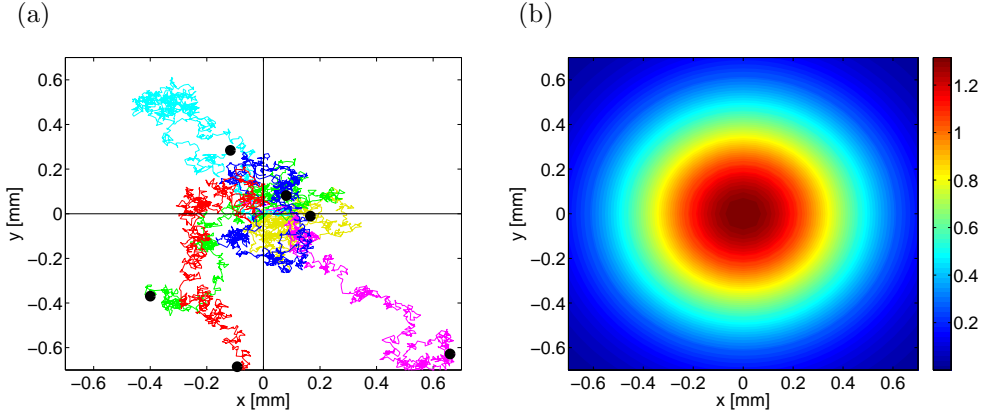


FIG. 3.1. (a) Six trajectories obtained by SSA (a6)–(b6) for $D = 10^{-4} \text{ mm}^2 \text{ sec}^{-1}$ and $\Delta t = 0.1 \text{ sec}$. Trajectories were started at the origin and followed for 10 minutes. (b) Probability distribution function $\psi(x, y, t)$ given by (3.5) at time $t = 10 \text{ min}$.

propensity functions which are changed by the chemical reaction which was selected in step (d5) of SSA (a5)–(d5). A more detailed discussion about the efficient computer implementation of the Gillespie SSA can be found e.g. in [16].

3. Diffusion. Diffusion is the random migration of molecules (or small particles) arising from motion due to thermal energy [3]. As shown by Einstein, the kinetic energy of a molecule (e.g. protein) is proportional to the absolute temperature. In particular, the protein molecule has a non-zero instantaneous speed at, for example, room temperature or at the temperature of the human body. A typical protein molecule is immersed in the aqueous medium of a living cell. Consequently, it cannot travel too far before it bumps into other molecules (e.g. water molecules) in the solution. As a result, the trajectory of the molecule is not straight but it executes a random walk as shown in Figure 3.1(a). We plot six possible trajectories of the protein molecule with six different colours. All trajectories start at the origin and are followed for 10 minutes. We will provide more details about this figure together with the methods for simulating molecular diffusion in the rest of this section. Stochastic models of diffusion which are based on the Smoluchowski equation are introduced in Section 3.1. In Section 3.2, we introduce a model which is suitable for coupling with the Gillespie SSA. Both modelling approaches will be used later in Section 4 for the stochastic modelling of reaction-diffusion processes. Let us note that there exist other models of molecular diffusion – they will be discussed in Section 6.

3.1. Smoluchowski equation and diffusion. Let $[X(t), Y(t), Z(t)] \in \mathbb{R}^3$ be the position of a diffusing molecule at time t . Starting with $[X(0), Y(0), Z(0)] = [x_0, y_0, z_0]$, we want to compute the time evolution of $[X(t), Y(t), Z(t)]$. To do that, we make use of a generator of random numbers which are normally distributed with zero mean and unit variance. Such a generator is part of many modern computer languages (e.g. function `randn` in Matlab). Diffusive spreading of molecules is characterised by a single *diffusion constant* D which depends on the size of the molecule, absolute temperature and viscosity of the solution [3]. Choosing time step Δt , we compute the time evolution of the position of the diffusing molecule by performing two steps at time t :

- (a6) Generate three normally distributed (with zero mean and unit variance) random numbers ξ_x , ξ_y and ξ_z .
 (b6) Compute the position of the molecule at time $t + \Delta t$ by

$$X(t + \Delta t) = X(t) + \sqrt{2D\Delta t} \xi_x, \quad (3.1)$$

$$Y(t + \Delta t) = Y(t) + \sqrt{2D\Delta t} \xi_y, \quad (3.2)$$

$$Z(t + \Delta t) = Z(t) + \sqrt{2D\Delta t} \xi_z, \quad (3.3)$$

Then continue with step (a6) for time $t + \Delta t$.

Choosing $D = 10^{-4} \text{ mm}^2 \text{ sec}^{-1}$ (diffusion constant of a typical protein molecule), $[X(0), Y(0), Z(0)] = [0, 0, 0]$ and $\Delta t = 0.1 \text{ sec}$, we plot six realizations of SSA (a6)–(b6) in Figure 3.1(a). We plot only the x and y coordinates. We follow the diffusing molecule for 10 minutes. The position of the molecule at time $t = 10 \text{ min}$ is denoted as a black circle for each trajectory.

Equations (3.1)–(3.3) are discretized versions of stochastic differential equations (SDEs) which are sometimes called Smoluchowski equations. Some basic facts about SDEs can be found e.g. in [2, 14]. A more accessible introduction to SDEs can be found in [23] which has a similar philosophy as our paper. Reference [23] is a nice algorithmic introduction to SDEs for students who do not have a prior knowledge of advanced probability theory or stochastic analysis. We will not go into details of SDEs in this paper, but only highlight some interesting facts which will be useful later.

First, equations (3.1)–(3.3) are not coupled. To compute the time evolution of $X(t)$, we do not need to know the time evolution of $Y(t)$ or $Z(t)$. We will later focus only on the time evolution of the x -th coordinate, effectively studying one-dimensional problems. Two-dimensional or three-dimensional problems can be treated similarly. Second, we see that different realizations of SSA (a6)–(b6) give different results. To get more reproducible quantities, we will shortly study the behaviour of several molecules. However, even in the case of a single diffusing molecule, there are still quantities whose evolution is deterministic. Let $\varphi(x, y, t) dx dy dz$ be the probability that $X(t) \in [x, x + dx)$, $Y(t) \in [y, y + dy)$ and $Z(t) \in [z, z + dz)$ at time t . It can be shown that φ evolves according to the partial differential equation

$$\frac{\partial \varphi}{\partial t} = D \left(\frac{\partial^2 \varphi}{\partial x^2} + \frac{\partial^2 \varphi}{\partial y^2} + \frac{\partial^2 \varphi}{\partial z^2} \right), \quad (3.4)$$

which is a special form of the so-called Fokker-Planck equation. Since our random walk starts at the origin, we can solve (3.4) with initial condition $\varphi(x, y, z, 0) = \delta(x, y, z)$ where δ is the Dirac distribution at the origin. We obtain

$$\varphi(x, y, z, t) = \frac{1}{(4D\pi t)^{3/2}} \exp \left[-\frac{x^2 + y^2 + z^2}{4Dt} \right].$$

In order to visualise this probability distribution function, we integrate it over z to get probability distribution function

$$\psi(x, y, t) = \int_{\mathbb{R}} \varphi(x, y, z, t) dz = \frac{1}{4D\pi t} \exp \left[-\frac{x^2 + y^2}{4Dt} \right]. \quad (3.5)$$

This means that $\psi(x, y, t) dx dy$ is the probability that $X(t) \in [x, x + dx)$ and $Y(t) \in [y, y + dy)$ at time t . The function $\psi(x, y, t)$ at time $t = 10 \text{ min}$ is plotted in Figure

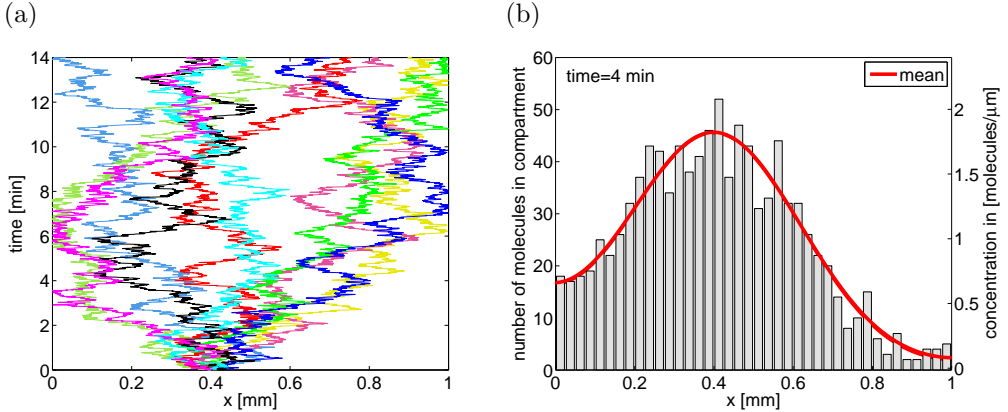


FIG. 3.2. (a) Ten trajectories computed by SSA (a7)–(c7) for $D = 10^{-4} \text{ mm}^2 \text{ sec}^{-1}$, $L = 1 \text{ mm}$, $X(0) = 0.4 \text{ mm}$ and $\Delta t = 0.1 \text{ sec}$. (b) Numbers of molecules in bins of length $h = 25 \text{ } \mu\text{m}$ at time $t = 4 \text{ min}$.

3.1(b). It can be obtained also by computing many realizations of SSA (a6)–(b6) and plotting the histogram of positions of a molecule at time 10 min; such positions were denoted as black circles for the six illustrative trajectories in Figure 3.1(a).

One important issue which was not addressed previously is that molecules diffuse in bounded volumes, i.e. the domain of interest has boundaries and suitable boundary conditions must be implemented. In the rest of this paper, we focus on one-dimensional problems to avoid technicalities. Hence, we effectively study diffusion of molecules in the one-dimensional interval $[0, L]$. Then the SSA can be formulated as follows:

(a7) Generate a normally distributed (with zero mean and unit variance) random number ξ .

(b7) Compute the position of the molecule at time $t + \Delta t$ by

$$X(t + \Delta t) = X(t) + \sqrt{2D \Delta t} \xi. \quad (3.6)$$

(c7) If $X(t + \Delta t)$ computed by (3.6) is less than 0, then

$$X(t + \Delta t) = -X(t) - \sqrt{2D \Delta t} \xi.$$

If $X(t + \Delta t)$ computed by (3.6) is greater than L , then

$$X(t + \Delta t) = 2L - X(t) - \sqrt{2D \Delta t} \xi.$$

Then continue with step (a7) for time $t + \Delta t$.

The boundary condition implemented in step (c7) is the so-called *reflective boundary condition* or zero flux boundary condition. It can be used when there is no chemical interaction between the boundary and diffusing molecules. More complicated boundary conditions are discussed in [7, 8].

Choosing $D = 10^{-4} \text{ mm}^2 \text{ sec}^{-1}$, $L = 1 \text{ mm}$, $X(0) = 0.4 \text{ mm}$ and $\Delta t = 0.1 \text{ sec}$, we plot ten realizations of SSA (a7)–(c7) in Figure 3.2(a). Let us assume that we have a system of 1000 molecules which are released at position $x = 0.4 \text{ mm}$ at time $t = 0$. Then Figure 3.2(a) can be viewed as a plot of the trajectories of ten representative molecules. Considering 1000 molecules, the trajectories of individual molecules are of no special interest. We are rather interested in spatial histograms (density of molecules). An example of such a plot is given in Figure 3.2(b). We simulate 1000

molecules, each following SSA (a7)–(c7). At time $t = 4$ min, we divided the domain of interest $[0, L]$ into 40 bins of length $h = L/40 = 25 \mu\text{m}$. We calculated the number of molecules in each bin $[(i-1)h, ih)$, $i = 1, 2, \dots, 40$, at time $t = 4$ min and plotted them as a histogram.

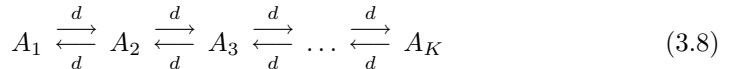
Let us note that the deterministic counterpart to the stochastic simulation is a solution of the corresponding Fokker-Planck equation (diffusion equation in our case) which, in one dimension with zero flux boundary conditions, reads as follows

$$\frac{\partial \varphi}{\partial t} = D \frac{\partial^2 \varphi}{\partial x^2} \quad \text{where} \quad \frac{\partial \varphi}{\partial x}(0) = \frac{\partial \varphi}{\partial x}(L) = 0. \quad (3.7)$$

The solution of (3.7) with the Dirac-like initial condition at $x = 0.4$ mm is plotted as a red solid line in Figure 3.2(b) for comparison.

3.2. Compartment-based approach to diffusion. In Section 3.1, we simulated the behaviour of 1000 molecules by computing the individual trajectories of every molecule (using SSA (a7)–(c7)). At the end of the simulation, we divided the computational domain $[0, L]$ into $K = 40$ compartments and we plotted numbers of molecules in each compartment in Figure 3.2(b). In particular, most of the computed information (1000 trajectories) was not used for the final result – the spatial histogram. We visualised only 40 numbers (numbers of molecules in compartments) instead of 1000 computed positions of molecules. In this section, we present a different SSA for the simulation of molecular diffusion. We redo the example from Section 3.1 but instead of simulating 1000 positions of the individual molecules, we are going to simulate directly the time evolution of 40 compartments.

To do that, we divide the computational domain $[0, L]$ into $K = 40$ compartments of length $h = L/K = 25 \mu\text{m}$. We denote the number of molecules of chemical species A in the i -th compartment $[(i-1)h, ih)$ by A_i , $i = 1, \dots, K$. We apply the Gillespie SSA to the following chain of “chemical reactions”:



where

$$A_i \xrightleftharpoons[d]{d} A_{i+1} \quad \text{means that} \quad A_i \xrightarrow{d} A_{i+1} \quad \text{and} \quad A_{i+1} \xrightarrow{d} A_i.$$

We will shortly show that the Gillespie SSA of (3.8) provides a correct model of diffusion provided that the rate constant d in (3.8) is chosen as $d = D/h^2$ where D is the diffusion constant and h is the compartment length. The compartment-based SSA can be described as follows. Starting with initial condition $A_i(t) = a_{0,i}$, $i = 1, 2, \dots, K$, we perform six steps at time t :

- (a8) Generate two random numbers r_1, r_2 uniformly distributed in $(0, 1)$.
- (b8) Compute propensity functions of reactions by $\alpha_i = A_i(t)d$ for $i = 1, 2, \dots, K$.
Compute

$$\alpha_0 = \sum_{i=1}^{K-1} \alpha_i + \sum_{i=2}^K \alpha_i. \quad (3.9)$$

- (c8) Compute the time at which the next chemical reaction takes place as $t + \tau$ where τ is given by (2.29).

(d8) If $r_2 < \sum_{i=1}^{K-1} \alpha_i / \alpha_0$, then find $j \in \{1, 2, \dots, K-1\}$ such that

$$r_2 \geq \frac{1}{\alpha_0} \sum_{i=1}^{j-1} \alpha_i \quad \text{and} \quad r_2 < \frac{1}{\alpha_0} \sum_{i=1}^j \alpha_i.$$

Then compute the number of molecules at time $t + \tau$ by

$$A_j(t + \tau) = A_j(t) - 1, \quad (3.10)$$

$$A_{j+1}(t + \tau) = A_{j+1}(t) + 1, \quad (3.11)$$

$$A_i(t + \tau) = A_i(t), \quad \text{for } i \neq j, i \neq j + 1. \quad (3.12)$$

(e8) If $r_2 \geq \sum_{i=1}^{K-1} \alpha_i / \alpha_0$, then find $j \in \{2, 3, \dots, K\}$ such that

$$r_2 \geq \frac{1}{\alpha_0} \left(\sum_{i=1}^{K-1} \alpha_i + \sum_{i=2}^{j-1} \alpha_i \right) \quad \text{and} \quad r_2 < \frac{1}{\alpha_0} \left(\sum_{i=1}^{K-1} \alpha_i + \sum_{i=2}^j \alpha_i \right).$$

Then compute the number of molecules at time $t + \tau$ by

$$A_j(t + \tau) = A_j(t) - 1, \quad (3.13)$$

$$A_{j-1}(t + \tau) = A_{j-1}(t) + 1, \quad (3.14)$$

$$A_i(t + \tau) = A_i(t), \quad \text{for } i \neq j, i \neq j - 1. \quad (3.15)$$

(f8) Continue with step (a8) for time $t + \tau$.

The first term on the right hand side of (3.9) corresponds to reactions $A_i \rightarrow A_{i+1}$ (jumps to the right) and the second term corresponds to reactions $A_i \rightarrow A_{i-1}$ (jumps to the left). The time of the next chemical reaction is computed in the step (c8) using formula (2.29) derived previously. The decision about which reaction takes place is done in steps (d8)–(e8) with the help of random number r_2 . Jumps to the right are implemented in step (d8) and jumps to the left in step (e8).

We want to redo the example from Section 3.1, i.e. simulate 1000 molecules starting from position 0.4 mm in the interval $[0, L]$ for $L = 1$ mm. We use $K = 40$. Since 0.4 mm is exactly a boundary between the 16th and 17th compartment, the initial condition is given by $A_{16}(0) = 500$, $A_{17}(0) = 500$ and $A_i(0) = 0$ for $i \neq 16$, $i \neq 17$. As $D = 10^{-4} \text{ mm}^2 \text{ sec}^{-1}$, we have $d = D/h^2 = 0.16 \text{ sec}^{-1}$. The numbers $A_i(t)$, $i = 1, \dots, K$, at time $t = 4$ min, are plotted in Figure 3.3(a) as a histogram. This panel can be directly compared with Figure 3.2(b). The computational intensity of SSA (a8)–(f8) can be decreased using the appropriate way to implement it in the computer. For example, only one chemical reaction occurs per time step. Consequently, only two propensity functions change and need to be updated in step (b8). Moreover, the formula (3.9) can be simplified as follows

$$\alpha_0 = \sum_{i=1}^{K-1} \alpha_i + \sum_{i=2}^K \alpha_i = 2 \sum_{i=1}^K \alpha_i - \alpha_1 - \alpha_K = 2d \sum_{i=1}^K A_i(t) - \alpha_1 - \alpha_K = 2dN - \alpha_1 - \alpha_K,$$

where $N = 1000$ is the total number of molecules in the simulation (this number is conserved because there is no creation or degradation of the molecules in the system). Hence, we need to recompute α_0 only when there is a change in α_1 or α_K , i.e. whenever the boundary compartments were involved in the previous reaction.

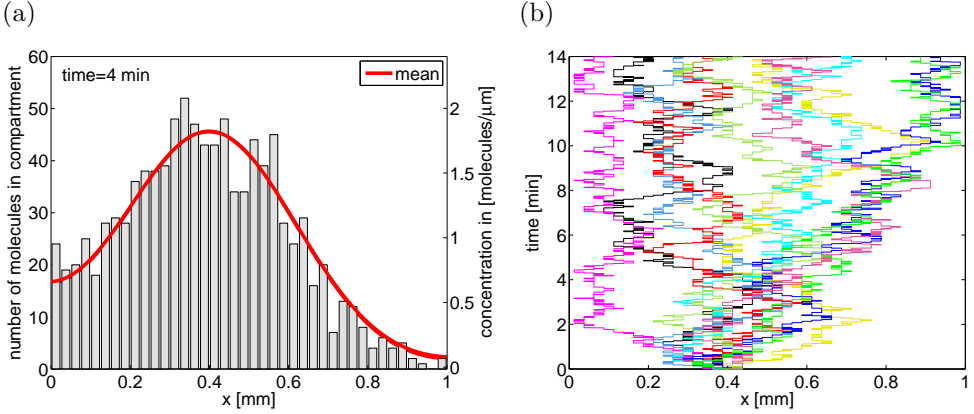


FIG. 3.3. *Compartment-based SSA model of diffusion.* (a) Numbers $A_i(t)$, $i = 1, 2, \dots, K$, at time $t = 4$ min obtained by SSA (a8)–(f8). We use $d = D/h^2 = 0.16 \text{ sec}^{-1}$, $K = 40$ and initial condition $A_{16}(0) = 500$, $A_{17}(0) = 500$ and $A_i(0) = 0$ for $i \neq 16, i \neq 17$. (b) Ten realizations of the simulation of an individual molecule by SSA (a8)–(f8).

SSA (a8)–(f8) does not compute the trajectories of individual molecules. However, we can still compute a plot comparable with Figure 3.2(a). To do that, we repeat the simulation with 1 molecule instead of 1000. Then, at given time t , exactly one of numbers $A_i(t)$, $i = 1, 2, \dots, K$, is non-zero and equal to 1. This is a position of the molecule at time t . Ten realizations of SSA (a8)–(f8) with one molecule released at 0.4 mm at $t = 0$ are plotted in Figure 3.3(b). This panel can be directly compared with Figure 3.2(a).

Let $p(\mathbf{n}, t)$ be the joint probability that $A_i(t) = n_i$, $i = 1, \dots, K$, where we denoted $\mathbf{n} = [n_1, n_2, \dots, n_K]$. Let us define operators $R_i, L_i : \mathbb{N}^K \rightarrow \mathbb{N}^K$ by

$$R_i : [n_1, \dots, n_i, n_{i+1}, \dots, n_K] \rightarrow [n_1, \dots, n_i + 1, n_{i+1} - 1, \dots, n_K], \quad i = 1, \dots, K-1, \quad (3.16)$$

$$L_i : [n_1, \dots, n_{i-1}, n_i, \dots, n_K] \rightarrow [n_1, \dots, n_{i-1} - 1, n_i + 1, \dots, n_K], \quad i = 2, \dots, K. \quad (3.17)$$

Then the chemical master equation, which corresponds to the system of chemical reactions given by (3.8), can be written as follows

$$\frac{\partial P(\mathbf{n})}{\partial t} = d \sum_{j=1}^{K-1} \left\{ (n_j + 1) P(R_j \mathbf{n}) - n_j P(\mathbf{n}) \right\} + d \sum_{j=2}^K \left\{ (n_j + 1) P(L_j \mathbf{n}) - n_j P(\mathbf{n}) \right\}. \quad (3.18)$$

The stochastic mean is defined as the vector $\mathbf{M}(t) \equiv [M_1, M_2, \dots, M_K]$ where

$$M_i(t) = \sum_{\mathbf{n}} n_i P(\mathbf{n}, t) \equiv \sum_{n_1=0}^{\infty} \sum_{n_2=0}^{\infty} \cdots \sum_{n_K=0}^{\infty} n_i P(\mathbf{n}, t) \quad (3.19)$$

gives the mean number of molecules in the i -th compartment, $i = 1, 2, \dots, K$. To derive an evolution equation for the stochastic mean vector $\mathbf{M}(t)$, we can follow the method from Section 2.2 – see derivation of (2.16) from chemical master equation (2.12). Multiplying (3.18) by n_i and summing over \mathbf{n} , we obtain (leaving the details

to the student) a system of equations for M_i of the form

$$\frac{\partial M_i}{\partial t} = d(M_{i+1} + M_{i-1} - 2M_i), \quad i = 2, \dots, K-1, \quad (3.20)$$

$$\frac{\partial M_1}{\partial t} = d(M_2 - M_1), \quad \frac{\partial M_K}{\partial t} = d(M_{K-1} - M_K). \quad (3.21)$$

System (3.20)–(3.21) is equivalent to a discretization of (3.7) provided that $d = D/h^2$. Hence, we have derived the relation between the rate constant d in (3.8), diffusion constant D and compartment length h . The solution of (3.7) with the Dirac-like initial condition at $x = 0.4$ mm is plotted for comparison as a red solid line in Figure 3.3(a).

The noise is described by the variance vector $\mathbf{V}(t) \equiv [V_1, V_2, \dots, V_K]$ where

$$V_i(t) = \sum_{\mathbf{n}} (n_i - M_i(t))^2 P(\mathbf{n}, t) \equiv \sum_{n_1=0}^{\infty} \sum_{n_2=0}^{\infty} \cdots \sum_{n_K=0}^{\infty} (n_i - M_i(t))^2 P(\mathbf{n}, t) \quad (3.22)$$

gives the variance of number of molecules in the i -th compartment, $i = 1, 2, \dots, K$. To derive the evolution equation for the vector $\mathbf{V}(t)$, we define the matrix $\{V_{i,j}\}$ by

$$V_{ij} = \sum_{\mathbf{n}} n_i n_j P(\mathbf{n}, t) - M_i M_j, \quad \text{for } i, j = 1, 2, \dots, K.$$

Using (3.22), we obtain $V_i = V_{ii}$ for $i = 1, 2, \dots, K$. Multiplying (3.18) by n_i^2 and summing over \mathbf{n} , we obtain

$$\begin{aligned} \frac{\partial}{\partial t} \sum_{\mathbf{n}} n_i^2 P(\mathbf{n}) &= d \sum_{j=1}^{K-1} \left\{ \sum_{\mathbf{n}} n_i^2 (n_j + 1) P(R_j \mathbf{n}) - \sum_{\mathbf{n}} n_i^2 n_j P(\mathbf{n}) \right\} \\ &\quad + d \sum_{j=2}^K \left\{ \sum_{\mathbf{n}} n_i^2 (n_j + 1) P(L_j \mathbf{n}) - \sum_{\mathbf{n}} n_i^2 n_j P(\mathbf{n}) \right\}. \end{aligned} \quad (3.23)$$

Let us assume that $i = 2, \dots, K-1$. Let us consider the term corresponding to $j = i$ in the first sum on the right hand side. We get

$$\begin{aligned} \sum_{\mathbf{n}} n_i^2 (n_i + 1) P(R_i \mathbf{n}) - \sum_{\mathbf{n}} n_i^2 n_i P(\mathbf{n}) &= \sum_{\mathbf{n}} (n_i - 1)^2 n_i P(\mathbf{n}) - \sum_{\mathbf{n}} n_i^2 n_i P(\mathbf{n}) \\ &= \sum_{\mathbf{n}} (-2n_i^2 + n_i) P(\mathbf{n}) = -2V_i - 2M_i^2 + M_i. \end{aligned}$$

First, we changed indices in the first sum $R_i \mathbf{n} \rightarrow \mathbf{n}$ and then we used definitions (3.19) and (3.22). Similarly, the term corresponding to $j = i-1$ in the first sum on the right hand side of (3.23) can be rewritten as

$$\begin{aligned} \sum_{\mathbf{n}} n_i^2 (n_{i-1} + 1) P(R_{i-1} \mathbf{n}) - \sum_{\mathbf{n}} n_i^2 n_{i-1} P(\mathbf{n}) &= \sum_{\mathbf{n}} (2n_i n_{i-1} + n_{i-1}) P(\mathbf{n}) \\ &= 2V_{i,i-1} + 2M_i M_{i-1} + M_{i-1}. \end{aligned}$$

Other terms (corresponding to $j \neq i, i-1$) in the first sum on the right hand side of (3.23) are equal to zero. The second sum can be handled analogously. We obtain

$$\begin{aligned} \frac{\partial}{\partial t} \sum_{\mathbf{n}} n_i^2 P(\mathbf{n}) &= d \left\{ 2V_{i,i-1} + 2M_i M_{i-1} + M_{i-1} - 2V_i - 2M_i^2 + M_i \right\} \\ &\quad + d \left\{ 2V_{i,i+1} + 2M_i M_{i+1} + M_{i+1} - 2V_i - 2M_i^2 + M_i \right\}. \end{aligned} \quad (3.24)$$

Using (3.22) and (3.20) on the left hand side of (3.24), we obtain

$$\frac{\partial}{\partial t} \sum_{\mathbf{n}} n_i^2 P(\mathbf{n}) = \frac{\partial V_i}{\partial t} + 2M_i \frac{\partial M_i}{\partial t} = \frac{\partial V_i}{\partial t} + d(2M_i M_{i+1} + 2M_i M_{i-1} - 4M_i^2).$$

Substituting this into (3.24), we get

$$\frac{\partial V_i}{\partial t} = 2d \left\{ V_{i,i+1} + V_{i,i-1} - 2V_i \right\} + d \left\{ M_{i+1} + M_{i-1} + 2M_i \right\} \quad (3.25)$$

for $i = 2, \dots, K-1$. Similarly, we get

$$\frac{\partial V_1}{\partial t} = 2d \left\{ V_{1,2} - V_1 \right\} + d \left\{ M_2 + M_1 \right\}, \quad (3.26)$$

$$\frac{\partial V_K}{\partial t} = 2d \left\{ V_{K,K-1} - V_K \right\} + d \left\{ M_{K-1} + M_K \right\}. \quad (3.27)$$

We see that the evolution equation for the variance vector $\mathbf{V}(t)$ depends on the mean \mathbf{M} , variance \mathbf{V} and on non-diagonal terms of the matrix $V_{i,j}$. To get a closed system of equations, we have to derive evolution equations for $V_{i,j}$ too. This can be done by multiplying (3.18) by $n_i n_j$, summing over \mathbf{n} and following the same arguments as before. We conclude this section with some consequences of (3.20)–(3.21) and (3.25)–(3.27). Looking at the steady states of equations (3.20)–(3.21), we obtain $M_i = N/K$, $i = 1, 2, \dots, K$, where N is the total number of diffusing molecules. Moreover, the variance equations imply that $V_i = N/K$, $i = 1, 2, \dots, K$, at the steady state.

4. Stochastic reaction-diffusion models. In this section, we add chemical reactions to both models of molecular diffusion which were presented in Section 3. We introduce two methods for the stochastic modelling of reaction-diffusion processes. The first one is based on the diffusion model from Section 3.2, the second one on the diffusion model from Section 3.1. We explain both methods using the same example. Namely, we consider molecules (e.g. protein) which diffuse in the domain $[0, L]$ with diffusion constant D as we considered in Section 3. Moreover, we assume that protein molecules are degraded (in the whole domain) and produced in part of the domain, i.e. we consider the chemical reactions from Sections 2.1 and 2.2 in our illustrative reaction-diffusion model. The model has a realistic motivation which is discussed in more detail later in Section 5.2. In Section 4.3, we present another illustrative example of a reaction-diffusion process incorporating the nonlinear model (2.27)–(2.28).

4.1. Compartment-based reaction-diffusion SSA. We consider molecules of chemical species A which are diffusing in the domain $[0, L]$, where $L = 1$ mm, with diffusion constant $D = 10^{-4}$ mm²sec⁻¹. Initially, there are no molecules in the system. Molecules are produced in the part of the domain $[0, L/5]$ with rate

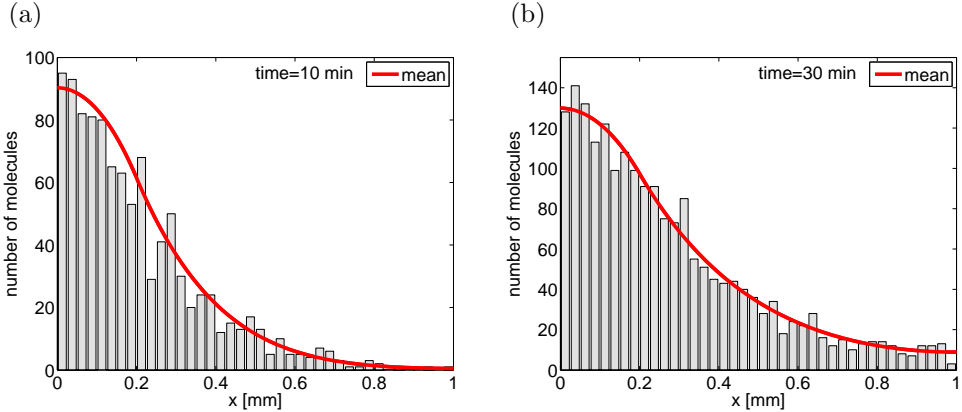
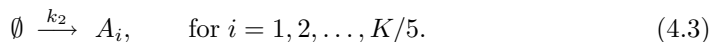
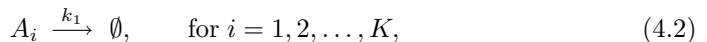
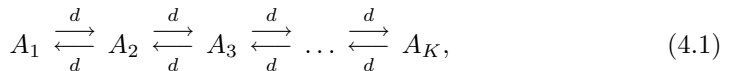


FIG. 4.1. One realization of the Gillespie SSA (a5)–(d5) for the system of chemical reactions (4.1)–(4.3). Gray histograms show numbers of molecules in compartments at time: (a) $t = 10$ min; (b) $t = 30$ min. Solution of (4.9)–(4.10) is plotted as the red solid line.

$k_p = 0.012 \mu\text{m}^{-1} \text{sec}^{-1}$. This means that the probability that a molecule is created in the subinterval of the length $1 \mu\text{m}$ is equal to $k_p dt$. Consequently, the probability that a molecule is created somewhere in the interval $[0, L/5]$ is equal to $k_p L/5 dt$. Molecules are degraded with rate $k_1 = 10^{-3} \text{sec}^{-1}$ according to the chemical reaction (2.1).

Following Section 3.2, we divide the computational domain $[0, L]$ into $K = 40$ compartments of length $h = L/K = 25 \mu\text{m}$. We denote the number of molecules of chemical species A in the i -th compartment $[(i-1)h, ih)$ by A_i , $i = 1, \dots, K$. Then our reaction-diffusion process is described by the system of chemical reactions



Equation (4.1) describes diffusion and is identical to (3.8). In particular, the rate constant d is given by $d = D/h^2$. Equation (4.2) describes the degradation of A and is, in fact, equation (2.1) applied to every compartment. Equation (4.3) describes the production of A in the first $K/5$ compartments (e.g. in part $[0, L/5]$ of the computational domain). The rate constant k_2 describes the rate of production per compartment. Since each compartment has length h , we have $k_2 = k_p h$.

The system of chemical reactions (4.1)–(4.3) is simulated using the Gillespie SSA (a5)–(d5). In our case, the propensity functions of reactions in (4.1) are given as $A_i(t)d$, the propensity functions of reactions in (4.2) are given as $A_i(t)k_1$ and propensity functions of reactions in (4.3) are equal to k_2 . Starting with no molecules of A in the system, we compute one realization of SSA (a5)–(d5) for the system of reactions (4.1)–(4.3). We plot the numbers of molecules in compartments at two different times in Figure 4.1.

Let $p(\mathbf{n}, t)$ be the joint probability that $A_i(t) = n_i$, $i = 1, \dots, K$, where we use the notation $\mathbf{n} = [n_1, n_2, \dots, n_K]$. Let us define operators $R_i, L_i : \mathbb{N}^K \rightarrow \mathbb{N}^K$ by (3.16)–(3.17). Then the chemical master equation, which corresponds to the system of chemical reactions (4.1)–(4.3), can be written as follows

$$\begin{aligned} \frac{\partial p(\mathbf{n})}{\partial t} = & d \sum_{i=1}^{K-1} \left\{ (n_i + 1) p(R_i \mathbf{n}) - n_i p(\mathbf{n}) \right\} + d \sum_{i=2}^K \left\{ (n_i + 1) p(L_i \mathbf{n}) - n_i p(\mathbf{n}) \right\} \\ & + k_1 \sum_{i=1}^K \left\{ (n_i + 1) p(n_1, \dots, n_i + 1, \dots, n_K) - n_i p(\mathbf{n}) \right\} \\ & + k_2 \sum_{i=1}^{K/5} \left\{ p(n_1, \dots, n_i - 1, \dots, n_K) - p(\mathbf{n}) \right\}. \end{aligned} \quad (4.4)$$

The first two sums correspond to diffusion (4.1), the third sum to degradation (4.2) and the fourth sum to production (4.3). The stochastic mean is defined as the vector $\mathbf{M}(t) \equiv [M_1, M_2, \dots, M_K]$ where M_i is given by (3.19). This gives the mean number of molecules in the i -th compartment, $i = 1, 2, \dots, K$, at time t (averaged over many realizations of SSA (a5)–(d5)). To derive the evolution equation for the stochastic mean vector $\mathbf{M}(t)$, we can follow the method from Section 2.2 – see derivation of (2.16) from the chemical master equation (2.12). Multiplying (4.4) by n_i and summing over all n_j , $j = 1, \dots, K$, we obtain (leaving the details to the student) a system of equations for M_i in the form

$$\frac{\partial M_1}{\partial t} = d(M_2 - M_1) + k_2 - k_1 M_1, \quad (4.5)$$

$$\frac{\partial M_i}{\partial t} = d(M_{i+1} + M_{i-1} - 2M_i) + k_2 - k_1 M_i, \quad i = 2, \dots, K/5, \quad (4.6)$$

$$\frac{\partial M_i}{\partial t} = d(M_{i+1} + M_{i-1} - 2M_i) - k_1 M_i, \quad i = K/5 + 1, \dots, K - 1, \quad (4.7)$$

$$\frac{\partial M_K}{\partial t} = d(M_{K-1} - M_K) - k_1 M_K. \quad (4.8)$$

System (4.5)–(4.8) is a discretized version of the reaction-diffusion equation

$$\frac{\partial a}{\partial t} = D \frac{\partial^2 a}{\partial x^2} + k_2 \chi_{[0, L/5]} - k_1 a \quad (4.9)$$

with zero-flux boundary conditions

$$\frac{\partial a}{\partial x}(0) = \frac{\partial a}{\partial x}(L) = 0. \quad (4.10)$$

Here, $\chi_{[0, L/5]}$ is the characteristic function of the interval $[0, L/5]$. Using initial condition $a(\cdot, 0) \equiv 0$, we computed the solution of (4.9)–(4.10) numerically. It is plotted as a red solid line in Figure 4.1 for comparison.

The concentration of molecules in the i -th compartment is defined as $\bar{M}_i = M_i/h$, $i = 1, \dots, K$. Dividing (4.5)–(4.8) by h , we can write a system of ODEs for \bar{M}_i . It is a discretized version of the reaction-diffusion equation

$$\frac{\partial \bar{a}}{\partial t} = D \frac{\partial^2 \bar{a}}{\partial x^2} + k_p \chi_{[0, L/5]} - k_1 \bar{a} \quad (4.11)$$

where $\bar{a} \equiv \bar{a}(x, t)$ is the concentration of molecules of A at point x and time t . The equation (4.11) provides a classical deterministic description of the reaction-diffusion process. Its parameters D , k_p and k_1 are independent of h . Solving (4.11) is equivalent to solving (4.9). Consequently, the red solid line in Figure 4.1 can be also viewed as a plot of $\bar{a}h$ where \bar{a} is the solution of the classical deterministic model (4.11) with the zero-flux boundary conditions.

4.2. Reaction-diffusion SSA based on the Smoluchowski equation.

In this section, we present a SSA which implements the Smoluchowski model of diffusion from Section 3.1, that is, we follow the trajectories of individual molecules. Diffusion of each molecule is modelled according to the model (a7)–(c7). We explain the SSA using the reaction-diffusion example from Section 4.1. Choosing a small time step Δt , we perform the following three steps at time t :

- (a9) For each molecule, compute its position at time $t + \Delta t$ according to steps (a7)–(c7).
- (b9) For each molecule, generate a random number r_1 uniformly distributed in the interval $(0, 1)$. If $r_1 < k_1 \Delta t$, then remove the molecule from the system.
- (c9) Generate a random number r_2 uniformly distributed in the interval $(0, 1)$. If $r_2 < k_p L/5 \Delta t$, then generate another random number r_3 uniformly distributed in the interval $(0, 1)$ and introduce a new molecule at position $r_3 L/5$. Continue with step (a9) for time $t + \Delta t$.

The degradation of molecules is modelled by step (b9). Equation (2.1) implies that $k_1 dt$ is the probability that a molecule is degraded in the time interval $[t, t + dt)$ for infinitesimally small dt . SSA (a9)–(c9) replaces dt by the finite time step Δt (compare with SSA (a1)–(b1)) which has to be chosen sufficiently small so that $k_1 \Delta t \ll 1$. Similarly, the probability that a molecule is created in $[0, L/5]$ in time interval $[t, t + dt)$ is equal to $k_p L/5 dt$. Consequently, we have to choose Δt so small that $k_p L/5 \Delta t$ is significantly less than 1. We choose $\Delta t = 10^{-2}$ sec. Then $k_1 \Delta t = 10^{-5}$ and $k_p L/5 \Delta t = 2.4 \times 10^{-2}$ for our parameter values $k_1 = 10^{-3} \text{ sec}^{-1}$, $k_p = 0.012 \mu\text{m}^{-1} \text{ sec}^{-1}$ and $L = 1 \text{ mm}$. Starting with no molecules of A in the system, we compute one realization of SSA (a9)–(c9). To visualise the results, we divide the interval $[0, L]$ into 40 bins and we plot the numbers of molecules in bins at time 10 minutes in Figure 4.2(a). The same plot at time 30 minutes is given in Figure 4.2(b). We used the same number of bins to visualise the results of SSA (a9)–(c9) as we used previously in the compartment-based model. Thus Figure 4.2 is directly comparable with Figure 4.1. We also plot the solution of (4.9)–(4.10) as a red solid line for comparison.

4.3. Reaction-diffusion models of nonlinear chemical kinetics.

In the previous sections, we studied an example of a reaction-diffusion model which did not include the second-order chemical reactions (2.26). We considered only production and degradation, i.e. we considered chemical reactions from Sections 2.1 and 2.2. In this section, we discuss generalisations of our approaches to models which involve second-order chemical reactions too. Our illustrative example is a reaction-diffusion process incorporating the nonlinear model (2.27)–(2.28). The second-order chemical reactions (2.26) require that two molecules collide (be close to each other) before the reaction can take place. The generalisation of SSA (a9)–(c9) to such a case is nontrivial and we will not present it in this paper (it can be found in [1]). Application of the Gillespie SSA (a5)–(d5) is more straightforward and is presented below.

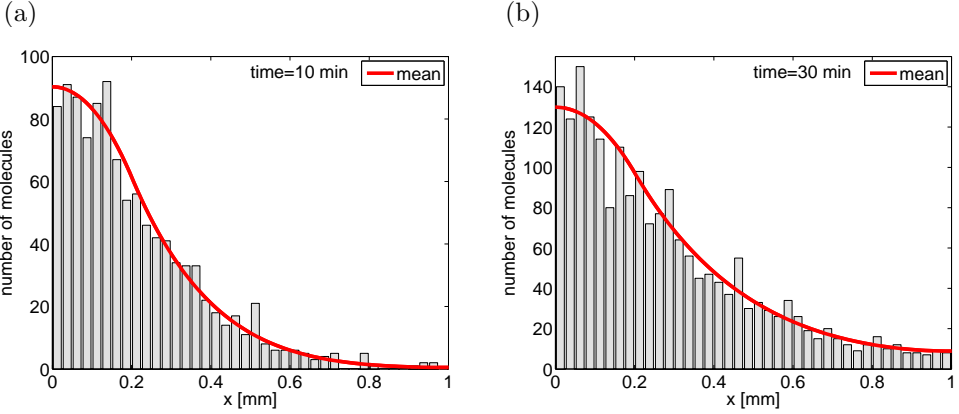
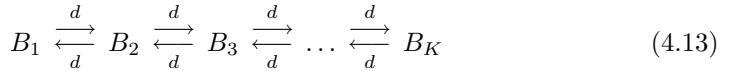
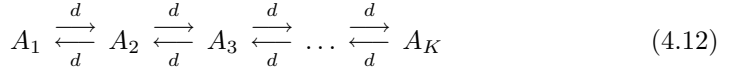
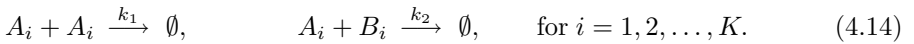


FIG. 4.2. One realization of SSA (a9)–(c9). Dividing domain $[0, L]$ into 40 bins, we plot the number of molecules in each bin at time: (a) $t = 10$ min; (b) $t = 30$ min. Solution of (4.9)–(4.10) is plotted as the red solid line.

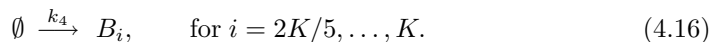
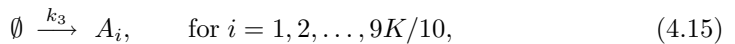
We consider that both chemical species A and B diffuse in the domain $[0, L]$, where $L = 1$ mm, with diffusion constant $D = 10^{-4}$ mm² sec⁻¹. Following the method of Section 4.1, we divide the computational domain $[0, L]$ into $K = 40$ compartments of length $h = L/K = 25$ μ m. We denote the number of molecules of chemical species A (resp. B) in the i -th compartment $[(i-1)h, ih)$ by A_i (resp. B_i), $i = 1, \dots, K$. Diffusion corresponds to two chains of “chemical reactions”:



Molecules of A and B are assumed to react according to chemical reactions (2.27) in the whole domain with rate constants $k_1 = 10^{-3}$ sec⁻¹ and $k_2 = 10^{-2}$ sec⁻¹ per one compartment, that is,



Production of chemical species (2.28) is assumed to take place only in parts of the computational domain $[0, L]$. Molecules of chemical species A (resp. B) are assumed to be produced in subinterval $[0, 9L/10]$ (resp. $[2L/5, L]$) with rate $k_3 = 1.2$ sec⁻¹ (resp. $k_4 = 1$ sec⁻¹) per one compartment of length h , that is,



Starting with no molecules in the system at time $t = 0$, we present one realization of the Gillespie SSA (a5)–(d5) applied to the chemical system (4.12)–(4.16) in Figure 4.3. We plot the numbers of molecules of A and B at time 30 minutes.

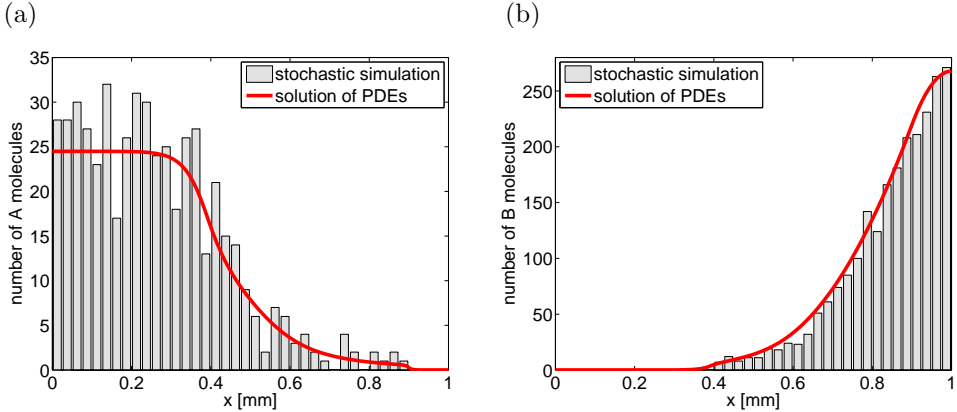


FIG. 4.3. One realization of the Gillespie SSA (a5)–(d5) for the system of chemical reactions (4.12)–(4.16). Numbers of molecules of chemical species A (left panel) and B (right panel) in compartments at time 30 minutes (gray histograms). Solution of (4.17)–(4.19) is plotted as the red solid line.

We already observed in Section 2.3 that the analysis of the master equation for chemical systems involving the second order reactions is not trivial. It is not possible to derive the equation for stochastic means as was done in Section 4.1 for the linear model. Hence, we will not attempt such an approach here. We also observed in Section 4.1 that the equation for the mean vector (4.5)–(4.8) was actually equal to a discretized version of the reaction-diffusion equation (4.9)–(4.10) which would be used as a traditional deterministic description. When considering the nonlinear chemical model (4.14)–(4.16), we cannot derive the equation for the mean vector but we can still write a deterministic system of partial differential equations (PDEs). We simply add diffusion to the system of ODEs (2.33)–(2.34) to obtain

$$\frac{\partial a}{\partial t} = D \frac{\partial^2 a}{\partial x^2} - 2k_1 a^2 - k_2 ab + k_3 \chi_{[0, 9L/10]}, \quad (4.17)$$

$$\frac{\partial b}{\partial t} = D \frac{\partial^2 b}{\partial x^2} - k_2 ab + k_4 \chi_{[2L/5, L]}, \quad (4.18)$$

and couple it with zero-flux boundary conditions

$$\frac{\partial a}{\partial x}(0) = \frac{\partial a}{\partial x}(L) = \frac{\partial b}{\partial x}(0) = \frac{\partial b}{\partial x}(L) = 0. \quad (4.19)$$

Using initial condition $a(\cdot, 0) \equiv 0$ and $b(\cdot, 0) \equiv 0$, we can compute the solution of (4.17)–(4.19) numerically. It is plotted as a red solid line in Figure 4.3 for comparison. We see that (4.17)–(4.19) gives a reasonable description of the system when comparing with one realization of SSA (a5)–(d5). However, let us note that solution of (4.17)–(4.19) is not equal to the stochastic mean.

The equations (4.17)–(4.19) can be also rewritten in terms of concentrations $\bar{a} = a/h$ and $\bar{b} = b/h$ as we did in the case of equations (4.9) and (4.11). Let us note that the rate constants scale with h as $k_1 = \bar{k}_1/h$, $k_2 = \bar{k}_2/h$, $k_3 = \bar{k}_3 h$, $k_4 = \bar{k}_4 h$ where $\bar{k}_1, \bar{k}_2, \bar{k}_3, \bar{k}_4$ are independent of h . Consequently, the equations for concentrations \bar{a} and \bar{b} are independent of h . They can be written in terms of the parameters $D, \bar{k}_1, \bar{k}_2, \bar{k}_3$ and \bar{k}_4 only (compare with (4.11)).

Finally, let us discuss the choice of the compartment length h . In Sections 3.2 and 4.1, we considered linear models and we were able to derive the equations for the mean vectors (e.g. (4.5)–(4.8)). Dividing (4.5)–(4.8) by h and passing to the limit $h \rightarrow 0$, we derive the corresponding deterministic reaction-diffusion PDE (4.11) which can be viewed (for linear models) as an equation for the probability distribution function of a single molecule (i.e. the exact description which we want to approximate by the compartment-based SSA). Consequently, we can increase the accuracy of the SSA by decreasing h . Considering the nonlinear model from this section, the continuum limit $h \rightarrow 0$ is not well-defined. The compartment-based SSA is generally considered valid only for a range of h values (i.e. the length h cannot be chosen arbitrarily small); conditions which the length h has to satisfy are subject of current research – see e.g. [24, Section 3.5].

5. Two important remarks. We explained SSAs for chemical reactions, molecular diffusion and reaction-diffusion processes in the previous sections. This final section is devoted to two important questions:

(a) Why do we care about stochastic modelling? The answer is given in Section 5.1 where we discuss connections between stochastic and deterministic modelling. In particular, we present examples where deterministic modelling fails and a stochastic approach is necessary. We start with a simple example of stochastic switching between favourable states of the system, a phenomenon which cannot be fully understood without stochastic modelling. Then we illustrate the fact that the stochastic model might have qualitatively different properties than its deterministic limit, i.e. the stochastic model is not just “equal” to the “noisy solution” of the corresponding deterministic equations. We present a simple system of chemical reactions for which the deterministic description converges to a steady state. On the other hand, the stochastic model of the same system of chemical reactions has oscillatory solutions. Finally, let us note that stochasticity plays important roles in biological applications, see e.g. [32, 6, 30].

(b) Why do we care about reaction-diffusion processes? The answer is given in Section 5.2 where we discuss biological pattern formation. Reaction-diffusion models are key components of models in developmental biology. We present stochastic analogues of two classical pattern forming models. The first one is the so-called French flag problem where we re-interpret the illustrative example from Sections 4.1 and 4.2. Then we present the reaction-diffusion pattern forming model based on the so-called Turing instability.

5.1. Deterministic vs. stochastic modelling. The models presented so far have one thing in common. One could use the deterministic description (given by ODEs or PDEs) and one would obtain a reasonable description of the system. In Sections 2.1, 2.2, 3.1, 3.2, 4.1 and 4.2, we studied linear models. We showed that the evolution equations for the stochastic mean are equal to (the discretized versions of) the corresponding deterministic differential equations. In Sections 2.3 and 4.3, we presented nonlinear models. We were not able to derive equations for the stochastic mean. However, we solved numerically the corresponding systems of deterministic equations (ODEs (2.33)–(2.34) in Section 2.3 and PDEs (4.17)–(4.19) in Section 4.3) and we obtained results comparable with the SSAs, i.e. results of the SSAs looked like “noisy solutions” of the corresponding differential equations. Here, we discuss examples of problems when SSAs give results which cannot be obtained by corresponding deterministic models.

Let us consider the model from Section 2.3. Its deterministic description is given

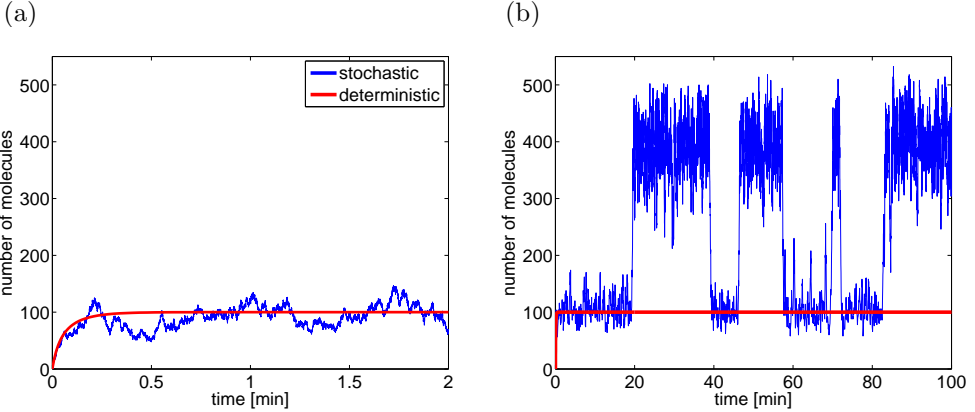
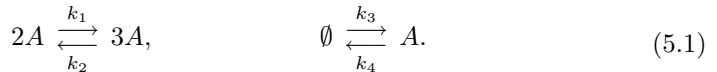


FIG. 5.1. *Simulation of (5.1). One realization of SSA (a5)–(d5) for the system of chemical reactions (5.1) (blue line) and the solution of the deterministic ODE (5.2) (red line). (a) The number of molecules of A as a function of time over the first two minutes of simulation. (b) Time evolution over 100 minutes.*

by the system of ODEs (2.33)–(2.34). Such a system has only one nonnegative (stable) steady state for our parameter values, namely $a_s = b_s = 10$. It can be observed from Figure 2.3 that solutions of (2.33)–(2.34) converge to a_s and b_s as $t \rightarrow \infty$. This is true for any nonnegative initial condition. The results of SSAs show fluctuation about the means, which are roughly equal to a_s and b_s (they are 9.6 for A and 12.2 for B). However, there are chemical systems which have two or more favourable states, so that the corresponding ODEs have more than one nonnegative stable steady state. For example, let us consider the system of chemical reactions for chemical A introduced by Schlögl [36]



The corresponding ODE is given as follows

$$\frac{da}{dt} = -k_2 a^3 + k_1 a^2 - k_4 a + k_3. \quad (5.2)$$

We choose the rate constants as follows: $k_1 = 0.18 \text{ min}^{-1}$, $k_2 = 2.5 \times 10^{-4} \text{ min}^{-1}$, $k_3 = 2200 \text{ min}^{-1}$ and $k_4 = 37.5 \text{ min}^{-1}$. Then the ODE (5.2) has two stable steady states $a_{s1} = 100$ and $a_{s2} = 400$ and one unstable steady state $a_u = 220$. The solution of (5.2) converges to one of the steady states with the choice of the steady state dependent on the initial condition. Let us consider that there are initially no molecules of A in the system, i.e. $A(0) = 0$. The solution of (5.2) is plotted in Figure 5.1(a) as a red line. We see that the solution of (5.2) converges to the stable steady state $a_{s1} = 100$. This is true for any initial condition $A(0) \in [0, a_u)$. If $A(0) > a_u$, then the solution of (5.2) converges to the second stable steady state $a_{s2} = 400$. Next, we use the Gillespie SSA (a5)–(d5) to simulate the chemical system (5.1). Starting with no molecules of A in the system, we plot one realization of SSA (a5)–(d5) in Figure 5.1(a) as a blue line. We see that the time evolution of A given by SSA (a5)–(d5) initially (over the first 2 minutes) looks like the noisy solution of (5.2). However, we can find significant differences between the stochastic and deterministic

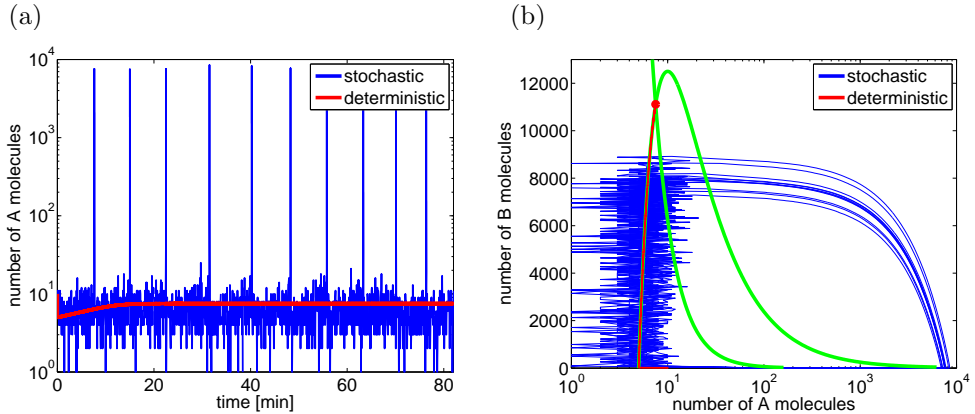
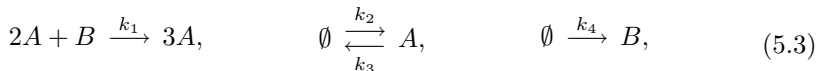


FIG. 5.2. *Self-induced stochastic resonance.* (a) One realization of SSA (a5)–(d5) for the system of chemical reactions (5.3) (blue line) and solution of the deterministic ODEs (red line). (b) Comparison of the stochastic and deterministic trajectories in the (A, B) -plane. Nullclines of the deterministic ODEs are plotted as green lines.

model if we observe both models over sufficiently large times – see Figure 5.1(b) where we plot the time evolution of A over the first 100 minutes. As expected, the solution of the deterministic model (5.2) stays forever close to the stable steady state $a_{s1} = 100$. The number of molecules given by the stochastic model initially fluctuates around one of the favourable states of the system (which is close to $a_{s1} = 100$). However, the fluctuations are sometimes so strong that the system spontaneously switches to another steady state (which is close to $a_{s2} = 400$). This random switching is missed by the deterministic description. If one wants to find the mean switching time between favourable states of the system, then it is necessary to implement SSAs. Random switching between states has been found in gene regulatory networks [15, 21]. Theoretical or computational approaches for the analysis of suitable stochastic models are given in [25, 9].

Our next example is a nonlinear system of chemical equations for which the stochastic model has qualitatively different behaviour than its deterministic counterpart in some parameter regimes. The presented phenomenon is sometimes called self-induced stochastic resonance [27]. Following an example from [5], we consider the system of chemical reactions introduced by Schnakenberg [37]



where we choose the rate constants as $k_1 = 4 \times 10^{-5} \text{ sec}^{-1}$, $k_2 = 50 \text{ sec}^{-1}$, $k_3 = 10 \text{ sec}^{-1}$ and $k_4 = 25 \text{ sec}^{-1}$. We use the Gillespie SSA (a5)–(d5) to simulate the time evolution of this system. To do that, let us note that the propensity function of the first reaction is equal to $A(t)(A(t) - 1)B(t)k_1$. We also derive and solve the deterministic system of ODEs corresponding to (5.3). Using the same initial conditions $[A, B] = [10, 10]$, we compare the results of the stochastic and deterministic models in Figure 5.2(a). We plot the time evolution of $A(t)$. We see that the solution of the deterministic equations converges to a steady state while the stochastic model has oscillatory solutions. Note that there is a log scale on the A -axis – numbers of A given by the (more precise) SSA vary between zero and ten thousand. If we use a linear

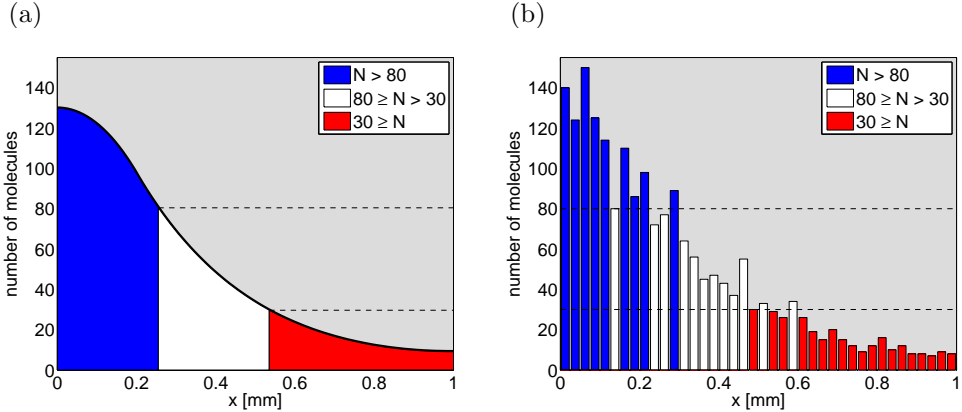


FIG. 5.3. *French flag problem.* (a) *Deterministic model.* (b) *Stochastic model.*

scale on the A -axis, then the low molecular fluctuations would be invisible and the solution of the SSAs would look as if there were “almost deterministic oscillations”, although it is the intrinsic noise which makes the oscillations possible. To understand this behaviour better, we plot the stochastic and deterministic trajectories in the (A, B) -plane in Figure 5.2(b). We include the nullclines of the deterministic system of ODEs (green lines). We see that the deterministic system follows a stable nullcline into the steady state (red circle). The stochastic model also initially “follows” this nullcline (with some noise) but it is the intrinsic noise which makes it possible for the stochastic model to leave the stable nullcline and oscillate (again we use a log scale on the A -axis).

5.2. Biological pattern formation. Reaction-diffusion processes are key elements of pattern forming mechanisms in developmental biology. The illustrative example from Sections 4.1 and 4.2 was a caricature of more complicated morphogenesis applications [38, 33] where one assumes that some prepatterning in the domain exists and one wants to validate the reaction-diffusion mechanism of the next stage of the patterning of the embryo. In our example, we considered a chemical A which is produced in part $[0, L/5]$ of domain $[0, L]$. Hence, the domain $[0, L]$ was divided into two different regions (prepatterning) $[0, L/5]$ and $[L/5, L]$. The simplest idea of further patterning is the so-called French flag problem [42]. We assume that the interval $[0, L]$ describes a layer of cells which are sensitive to the concentration of chemical A . Let us assume that a cell can have three different fates (e.g. different genes are switched on or off) depending on the concentration of chemical A . Then the concentration gradient of A can help to distinguish three different regions in $[0, L]$ – see Figure 5.3. If the concentration of A is high enough (above a certain threshold), a cell follows the first possible program (denoted blue in Figure 5.3). The “white program” (resp. “red program”) is followed for medium (resp. low) concentrations of A . The deterministic version of the French flag problem is presented in Figure 5.3(a). We consider a solution of (4.9)–(4.10) at time 30 minutes which is the red curve in Figure 4.1(b) or Figure 4.2(b). The solution of (4.9)–(4.10) is decreasing in space. Introducing two thresholds, we can clearly obtain three well-defined regions as seen in Figure 5.3(a). The stochastic version of the French flag problem is presented in Figure 5.3(b). We take the spatial histogram presented in Figure 4.2(b). We introduce two thresholds (80 and 30 molecules) as before and replot the histogram using the corre-

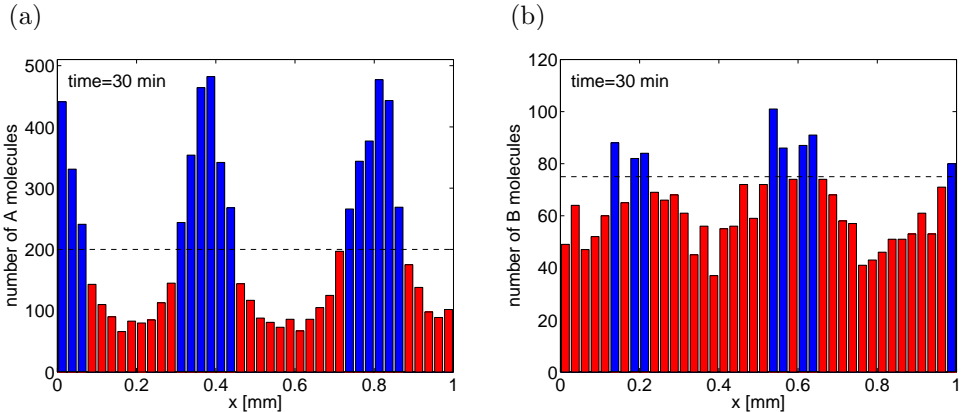


FIG. 5.4. Turing patterns. (a) Numbers of molecules of chemical species A in each compartment at time 30 minutes; (b) the same plot for chemical species B .

sponding colours. Clearly, the resulting “French flag” is noisy. Different realizations of the SSA would lead to different noisy French flags. The same is true for the SSA from Figure 4.1(b).

Our second example of patterning in developmental biology are the so-called Turing patterns [41, 17, 28, 39]. They do not require any prepatterning. Molecules are subject to the same chemical reactions in the whole domain of interest. For example, let us consider a system of two chemical species A and B which react according to the Schnakenberg system of chemical reactions (5.3). Let us choose the values of rate constants as $k_1 = 10^{-6} \text{ sec}^{-1}$, $k_2 = 1 \text{ sec}^{-1}$, $k_3 = 0.02 \text{ sec}^{-1}$ and $k_4 = 3 \text{ sec}^{-1}$. The corresponding deterministic system of ODEs for (5.3) has one nonnegative stable steady state equal to $a_s = 200$ and $b_s = 75$ molecules. Introducing diffusion to the model, one steady state solution of the spatial problem is the constant one (a_s, b_s) everywhere. However, such a solution might not be stable (i.e. might not exist in reality) if the diffusion constants of A and B differ significantly. We choose $D_A = 10^{-5} \text{ mm}^2 \text{ sec}^{-1}$ and $D_B = 10^{-3} \text{ mm}^2 \text{ sec}^{-1}$, i.e. $D_B/D_A = 100$. To simulate the reaction-diffusion problem with the Schnakenberg system of chemical reactions (5.3), we follow the method of Section 4.1. We divide the computational domain $[0, L]$ into $K = 40$ compartments of length $h = L/K = 25 \mu\text{m}$. We denote the number of molecules of chemical species A (resp. B) in the i -th compartment $[(i-1)h, ih]$ by A_i (resp. B_i), $i = 1, \dots, K$. Diffusion is described by two chains of chemical reactions (4.12)–(4.13) where the rates of “chemical reactions” are equal to $d_A = D_A/h^2$ for chemical species A and $d_B = D_B/h^2$ for chemical species B . Chemical reactions (5.3) are considered in every compartment (the values of rate constants in (5.3) are already assumed to be expressed in units per compartment). Starting with a uniform distribution of chemicals $A_i(0) = a_s = 200$ and $B_i(0) = b_s = 75$, $i = 1, 2, \dots, K$, at time $t = 0$, we plot the numbers of molecules in each compartment at time $t = 30$ minutes computed by SSA (a5)–(d5) in Figure 5.4. To demonstrate the idea of patterning, compartments with many molecules (above steady state values a_s or b_s) are plotted as blue; other compartments are plotted as red. We see in Figure 5.4(a) that chemical A can be clearly used to divide our computational domain into several regions. There are two and half blue peaks in this figure. The number of blue peaks depends on the size of the computational domain $[0, L]$ and it is not a unique number

in general. The reaction-diffusion system has several favourable states with a different number of blue peaks. As discussed in Section 5.1, the solution of the corresponding deterministic model converges to one of the favourable (stable steady) states of the system. The stochastic model enables stochastic switching between the favourable states, i.e. between the states with a different number of blue peaks.

6. Discussion. We presented SSAs for systems of chemical reactions and molecular diffusion. Then we presented methods for simulating both reactions and diffusion at the same time. The algorithms for simulating (spatially homogeneous) systems of chemical reactions were based on the work of Gillespie [18]. We did not focus on the computer implementation of the algorithms. We chose simple examples which can be simulated quickly. If one considers systems of many equations, there are ways to make the Gillespie SSA more efficient [16]. For example, it would be a waste of time to recompute all the propensity functions at each time step. We simulate one reaction per one time step. Therefore, it makes sense to update only those propensity functions which are changed by the chemical reaction which was selected in step (d5) of SSA (a5)–(d5).

We only briefly touched on the concept of the Fokker-Planck equation [34] when we discussed the Smoluchowski description of diffusion. It is worth noting that there are interesting connections between the chemical master equation (which is equivalent to the Gillespie SSA) and the Fokker-Planck equation which gives the time evolution of the probability distribution. Such connections are discussed (through the so-called chemical Langevin equation) in [20]. The Smoluchowski equation is actually the same mathematical object as the chemical Langevin equation, i.e. the stochastic differential equation [2]. An algorithmic introduction to stochastic differential equations can be found in [23].

We presented two models of diffusion in this paper. One was based on the chain of “chemical reactions” (3.8) computing the time evolution of the numbers of molecules in compartments. Coupling this model with the modelling of chemical reactions is straightforward and presented in Section 4.1; such a compartment-based approach is used e.g. in [40, 24, 22]. The second model for molecular diffusion was based on the Smoluchowski equation (3.6). It was an example of the so-called position jump process, that is, a molecule jumps to a different location at each time step. As a result, the trajectory of a molecule is discontinuous. The individual trajectories of diffusing molecules can be also modelled using the so-called velocity jump processes [29], that is, the position of a molecule $x(t)$ follows the deterministic equation $dx/dt = v$ where $v(t)$, the velocity of the molecule, changes stochastically. Such stochastic processes can be used not only for the simulation of diffusing molecules but also for the description of movement of unicellular organisms like bacteria [10, 11] or amoeboid cells [12]. Velocity jump processes can be also described in terms of PDEs for the time evolution of the probability distributions to find a particle (molecule or cell) at a given place. Such equations are not exactly equal to the diffusion equation. However, they can be reduced in the appropriate limit to the diffusion equation [43, 7]. A classical review paper on diffusion and other stochastic processes was written by Chandrasekhar [4], a nice introduction to random walks in biology is the book by Berg [3].

In this paper, we used only reflective boundary conditions, that is, particles hitting the boundary were reflected back. Such boundary conditions are suitable whenever there is no chemical interaction between molecules in the solution and the boundary of the domain. Considering biological applications, it is often the case that molecules (e.g. proteins) react with the boundary (e.g. with receptors in the cellular mem-

brane). Then the boundary conditions have to be modified accordingly. It has to be assumed that some molecules which hit the boundary are reflected and some molecules are adsorbed by the boundary (e.g. become bound to the receptor or take part in membrane-based chemical reactions). The probability that a molecule is adsorbed rather than reflected depends on the chemical properties of the boundary and also on the SSA which is used for modelling (further details are given in [7, 8]).

Our analysis of SSAs was based on the chemical master equation. We successfully derived equations for the means and variances in illustrative examples which did not include second-order reactions. Other first-order reaction networks can be also analysed using this framework [13]. The nonlinear chemical kinetics complicates the mathematical analysis significantly. We can write a deterministic description but it might be too far from the correct description of the system [35]. A review of more computational approaches for the analysis of SSAs can be found in [26]. Applications of such methods to stochastic reaction-diffusion processes is presented in [31].

Acknowledgements. This work was supported by the Biotechnology and Biological Sciences Research Council (grant ref. BB/C508618/1), St. John's College, Oxford and Linacre College, Oxford (RE). Authors would like to give thanks for helpful suggestions and encouraging comments during the preparation of this manuscript to Ruth Baker, Hyung Ju Hwang, Chang Hyeong Lee, Hans Othmer, Jan Rychtar and Aidan Twomey.

REFERENCES

- [1] S. Andrews and D. Bray, *Stochastic simulation of chemical reactions with spatial resolution and single molecule detail*, *Physical Biology* **1** (2004), 137–151.
- [2] L. Arnold, *Stochastic Differential Equations, theory and applications*, Wiley-Interscience Publication, 1974.
- [3] H. Berg, *Random Walks in Biology*, Princeton University Press, 1983.
- [4] S. Chandrasekhar, *Stochastic problems in physics and astronomy*, *Reviews of Modern Physics* **15** (1943), 2–89.
- [5] R. DeVille, C. Muratov, and E. Vanden-Eijnden, *Non-meanfield deterministic limits in chemical reaction kinetics*, *Journal of Chemical Physics* **124** (2006), 231102.
- [6] M. Elowitz, A. Levine, E. Siggia, and P. Swain, *Stochastic gene expression in a single cell*, *Science* **297** (2002), 1183–1186.
- [7] R. Erban and S. J. Chapman, *Reactive boundary conditions for stochastic simulations of reaction-diffusion processes*, *Physical Biology* **4** (2007), no. 1, 16–28.
- [8] ———, *Time scale of random sequential adsorption*, *Physical Review E* **75** (2007), no. 4, 041116.
- [9] R. Erban, I. Kevrekidis, D. Adalsteinsson, and T. Elston, *Gene regulatory networks: A coarse-grained, equation-free approach to multiscale computation*, *Journal of Chemical Physics* **124** (2006), 084106.
- [10] R. Erban and H. Othmer, *From individual to collective behaviour in bacterial chemotaxis*, *SIAM Journal on Applied Mathematics* **65** (2004), no. 2, 361–391.
- [11] ———, *From signal transduction to spatial pattern formation in E. coli: A paradigm for multiscale modeling in biology*, *Multiscale Modeling and Simulation* **3** (2005), no. 2, 362–394.
- [12] ———, *Taxis equations for amoeboid cells*, *Journal of Mathematical Biology* **54** (2007), no. 6, 847–885.
- [13] C. Gadgil, C. Lee, and H. Othmer, *A stochastic analysis of first-order reaction networks*, *Bulletin of Mathematical Biology* **67** (2005), 901–946.
- [14] G.W. Gardiner, *Handbook of Stochastic Processes for physics, chemistry and natural sciences*, 2 ed., Springer Verlag, 1985.
- [15] T. Gardner, C. Cantor, and J. Collins, *Construction of a genetic toggle switch in E. coli*, *Nature* **403** (2000), 339–342.
- [16] M. Gibson and J. Bruck, *Efficient exact stochastic simulation of chemical systems with many species and many channels*, *Journal of Physical Chemistry A* **104** (2000), 1876–1889.

- [17] A. Gierer and H. Meinhardt, *A theory of biological pattern formation*, Kybernetik **12** (1972), 30–39.
- [18] D. Gillespie, *Exact stochastic simulation of coupled chemical reactions*, Journal of Physical Chemistry **81** (1977), no. 25, 2340–2361.
- [19] ———, *Markov Processes, an introduction for physical scientists*, Academic Press, Inc., Harcourt Brace Jovanovich, 1992.
- [20] ———, *The chemical Langevin equation*, Journal of Chemical Physics **113** (2000), no. 1, 297–306.
- [21] J. Hastay, D. McMillen, and J. Collins, *Engineered gene circuits*, Nature **420** (2002), 224–230.
- [22] J. Hattne, D. Fange, and J. Elf, *Stochastic reaction-diffusion simulation with MesoRD*, Bioinformatics **21** (2005), no. 12, 2923–2924.
- [23] D.J. Higham, *An algorithmic introduction to numerical simulation of stochastic differential equations*, SIAM Review **43** (2001), no. 3, 525–546.
- [24] S. Isaacson and C. Peskin, *Incorporating diffusion in complex geometries into stochastic chemical kinetics simulations*, SIAM Journal on Scientific Computing **28** (2006), no. 1, 47–74.
- [25] T. Kepler and T. Elston, *Stochasticity in transcriptional regulation: Origins, consequences and mathematical representations*, Biophysical Journal **81** (2001), 3116–3136.
- [26] I. Kevrekidis, C. Gear, J. Hyman, P. Kevrekidis, O. Runborg, and K. Theodoropoulos, *Equation-free, coarse-grained multiscale computation: enabling microscopic simulators to perform system-level analysis*, Communications in Mathematical Sciences **1** (2003), no. 4, 715–762.
- [27] C. Muratov, E. Vanden-Eijnden, and W. E, *Self-induced stochastic resonance in excitable systems*, Physica D **210** (2005), 227–240.
- [28] J. Murray, *Mathematical Biology*, Springer Verlag, 2002.
- [29] H. Othmer, S. Dunbar, and W. Alt, *Models of dispersal in biological systems*, Journal of Mathematical Biology **26** (1988), 263–298.
- [30] J. Paulsson, O. Berg, and M. Ehrenberg, *Stochastic focusing: Fluctuation-enhanced sensitivity of intracellular regulation*, Proceedings of the National Academy of Sciences USA **97** (2000), no. 13, 7148–7153.
- [31] L. Qiao, R. Erban, C. Kelley, and I. Kevrekidis, *Spatially distributed stochastic systems: Equation-free and equation-assisted preconditioned computation*, Journal of Chemical Physics **125** (2006), 204108.
- [32] C. Rao, D. Wolf, and A. Arkin, *Control, exploitation and tolerance of intracellular noise*, Nature **420** (2002), 231–237.
- [33] G. Reeves, R. Kalifa, D. Klein, M. Lemmon, and S. Shvartsman, *Computational analysis of EGFR inhibition by Argos*, Developmental biology **284** (2005), 523–535.
- [34] H. Risken, *The Fokker-Planck Equation, methods of solution and applications*, Springer-Verlag, 1989.
- [35] M. Samoilov and A. Arkin, *Deviant effects in molecular reaction pathways*, Nature Biotechnology **24** (2006), no. 10, 1235–1240.
- [36] F. Schlögl, *Chemical reaction models for non-equilibrium phase transitions*, Zeitschrift für Physik **253** (1972), no. 2, 147–161.
- [37] J. Schnakenberg, *Simple chemical reaction systems with limit cycle behaviour*, Journal of Theoretical Biology **81** (1979), 389–400.
- [38] O. Shimmi, D. Umulis, H. Othmer, and M. Connor, *Facilitated transport of a Dpp/Scw heterodimer by Sog/Tsg leads to robust patterning of the Drosophila blastoderm embryo*, Cell **120** (2005), no. 6, 873–886.
- [39] S. Sick, S. Reinker, J. Timmer, and T. Schlake, *WNT and DKK determine hair follicle spacing through a reaction-diffusion mechanism*, Science **314** (2006), 1447–1450.
- [40] A. Stundzia and C. Lumsden, *Stochastic simulation of coupled reaction-diffusion processes*, Journal of Computational Physics **127** (1996), 196–207.
- [41] A. Turing, *The chemical basis of morphogenesis*, Phil. Trans. Roy. Soc. Lond. **237** (1952), 37–72.
- [42] L. Wolpert, R. Beddington, T. Jessel, P. Lawrence, E. Meyerowitz, and J. Smith, *Principles of Development*, Oxford University Press, 2002.
- [43] E. Zauderer, *Partial Differential Equations of Applied Mathematics*, John Wiley & Sons, 1983.